Manuscript

Journal of Engineering Mechanics, Volume 145, Issue 12, December 2019
DOI:10.1061/(ASCE)EM.1943-7889.0001674

Piezoelectric Metamaterial with Negative and Zero Poisson's Ratio

Khan, K.A.[1*], Al-Mansoor, S[2], Khan, S.Z[3], Khan, M.A[4]

[1]Department of Aerospace Engineering, Khalifa University of Science and Technology, Abu Dhabi, UAE

[2]Department of Aerospace Engineering, Khalifa University of Science and Technology, Abu Dhabi, UAE

[3]Department of Mechanical Engineering, Islamic University of Madinah, Madinah, Saudi Arabia

[4]School of Aerospace, Transport and Manufacturing, Cranfield University, UK

Abstract

This study presents the finite-element based micromechanical modeling approach to obtain the electromechanical properties of the piezoelectric metamaterial based on honeycomb (HC) cellular networks. The symmetry of the periodic structure was employed to derive mixed boundary conditions (MBCs) analogous to PBCs. Three classes of hexagonal HC cellular networks, namely, conventional HC (CHC), a re-entrant HC (RE) and a semi-re-entrant HC (SRE) were considered. The representative volume elements (RVEs) of these three classes of cellular materials were created, and finite element analyses were carried out in order to analyze the effect of orientation of the ligament on their effective electromechanical properties and their suitability in specific engineering applications. The longitudinally poled piezoelectric HC cellular networks showed an enhanced behavior as compared to the monolithic piezoelectric materials. Moreover, longitudinally poled HC cellular networks demonstrated that, as compared to the bulk constituent, their hydrostatic figure of merit increased and their and acoustic impedance decreased by one order of magnitude, respectively, indicating their applicability for the design on hydrophones. Moreover, results showed that cellular metamaterial with tunable electromechanical characteristics and variety of auxetic behaviors such as negative, positive or zero Poisson's ratios could be

* Corresponding author. Tel.: +971-(02) 4018227; Fax: +971-(02) 4472442
E-mail address: kamran.khan@ku.ac.ae (K.A. Khan)

developed. Such novel HC network-based functional cellular materials likely to facilitate the design of light-weight devices for various next-generation sensors and actuators.

Keywords: cellular materials; effective electromechanical response, honeycomb cellular networks, micromechanical modeling, piezoelectric materials, smart auxetic structures.

Introduction

Piezoelectric materials (PMs) play a key role in advanced multifunctional composites industry by virtue of their unique electromechanical coupling characteristics (Muliana 2011). PMs have found applications in actuators, sensors, ultrasound imagers, hydrophones and echo-cardiogram (Marselli et al. 1999). In these devices, PMs convert mechanical energy into electrical or vice-versa. For example, in sensing applications, PMs require high sensitivity and low acoustic impedance (Alkhader et al. 2015; Lethiecq et al. 2004). Existing bulk piezoelectric polymers show low acoustic impedance and sensitivity while ceramics type piezoelectric materials have high acoustic impedance and sensitivity (Kar-Gupta and Venkatesh 2006). Several studies were conducted to enrich the coupling characteristics between the mechanical and electrical properties in piezoelectric materials by either embedding constituents (Topolov and Bowen 2008) or by introducing the porosity (Hikita et al. 1983).

Piezoelectric composites were tailored to exhibit improved piezoelectric activity and mechanical flexibility (for example, active fiber composites, AFM) (Elhajjar et al. 2013). However, the porosity can significantly enhance the performances of medical diagnostic devices (Smith 1989) and hydrophones (Geis et al. 2000). Both piezoelectric composites (e.g., (Skinner et al. 1978); (Ramesh et al. 2006); (Richard et al. 2004))., and porous PMs (e.g., Nagata et al. 1980; Hikita et al. 1983; Ting 1985; Bast and Wersing 1989; Bowen et al. 2004; Piazza et al. 2005; Zhang et al. 2007; Lee et al. 2007) showed potential in obtaining low acoustic impedance and high piezoelectric

sensitivity. However, currently, piezoelectric composites demonstrate properties far from the ideal electromechanical characteristics.

In designing the porous PMs and the piezoelectric composites, the spatial distribution of the two phases controls the effective enhancement of the electromechanical properties (Levassort et al. 1998). Therefore, the concept of phase connectivity was defined (Newnham et al. 1978). To understand the role of connectivity of porosity on the properties of PMs, several experimental studies were conducted by considering numerous configurations of porosity, such as, embedded porosity in a PMs (3-0 foam) (Marselli et al. 1999; Kara et al. 2003; Ueda et al. 2010); long cylinder-like porosity (3-1 foam) (Wirges et al. 2007) and open-cell like porosity (3-3 foam) (Nagata et al. 1980). Results demonstrated that porosity help to enhance the sensitivity of PMs.

Several analytical studies were conducted to estimate the electromechanical characteristics of porous PMs by considering simplified configurations of porosity (such as 3-0 and 3-1) (Banno 1985, Dunn and Taya 1993b, Mikata 2001, Bowen and Topolov 2003). Several micromechanical models based finite element frameworks were developed for predicting electromechanical properties of 3-0, 3-1 and 3-3 type porous PMs and hence addressed more complex microstructure (Kar-Gupta and Venkatesh 2008, Bosse et al. 2012). These studies established that behavior of porous PMs governed by the porosity level, pore shape, pore direction, and their distribution, cellular interconnectivity and the direction of the poling (Iyer et al. 2015)**.**

Piezoelectric cellular materials (e.g., Challagulla and Venkatesh 2012, Bauer et al. 2014) and piezoelectric architectured foams (Fang et al. 2007; Ueda et al. 2010) are the possible subclasses of the porous PMs. These subclasses can be used to tailor the microstructure for developing novel materials with the desired multifunctionality for specific applications (Wadley 2006).

Among Piezoelectric cellular solids and architectured foams, the 3-1 type cellular honeycomb (HC) configuration is highly in use due to its simplicity, utility, and workability with structures. Based on the ligament orientations the HC architecture may produce deformation with positive (conventional), negative (auxetic) and zero Poisson ratio's (Grima et al. 2010). Auxetic materials are attractive due to their counterintuitive response under deformation and improved properties. The structural behavior of HC cellular networks with passive elastic anisotropic ligaments representing auxetic effects has been extensively studied (Grima et al. 2010, Masters and Evans 1996, Gibson and Ashby 1997, Zhu et al. 1997). These studies established that the ligament orientation of cellular network governed the hexagonal HC architecture-property relationship (Alkhader and Vural 2009; Papka and Kyriakides 1999).

In the case of the PMs with cellular networks, there is an auxiliary complexity in finding out optimized architecture-property relationship due to the electromechanical coupling parameters. The dielectric, elastic, and electromechanical coupling anisotropy of the ligament base material, the orientation of the poling direction are the main features of the mentioned problem. There is no analytical model available in the literature that could yield the electromechanical properties of the piezoelectric HC cellular network. Moreover, the relationship between the overall electromechanical properties and the microstructure features for the complete family of piezoelectric HC cellular networks is still not available. Recent experimental work on the fabricated 3-1 type auxetic lattice structure from bulk PZT piezo-ceramic showed promising electromechanical properties with negative in-plane Poisson's ratio of -2.05 (Fey et al. 2016). These experimental findings motivate the present study.

97 In this paper, micromechanical modeling based FE computational framework is proposed to
98 characterize the effects of poling direction, anisotropic material behavior and ligament orientation
99 on the electromechanical properties of piezoelectric hexagonal HC cellular solids.

100 **Architecture of Piezoelectric Cellular Material**

101 We have considered three types of HC piezoelectric architected materials as shown in Figure
102 1. These included conventional hexagonal HC structure (CHC), a re-entrant HC (RE) (which
103 generates auxetic behavior) and a semi-re-entrant HC (SRE). In specific configurations, the
104 proposed HC cellular networks can yield a variety of auxetic behavior, i.e., positive, negative and
105 zero Poisson's ratio.

106 Figure 1 shows the proposed architectures and the four parameters that are used to describe the
107 geometry of HC cellular network. The parameters h, l, t, and θ are referred to as the height of
108 vertical rib, the angular rib length, the rib thickness, and the rib angle, respectively, as shown in
109 the unit cell (UC) of each HC network in Figure 1. We fixed the h=10mm, l=4mm, t=1mm. To
110 obtain different auxetic behaviors, the orientations of the ligaments (θ) of the cellular network
111 were varied as shown in the corresponding unit cell (UC). The HC cellular network ligament
112 material is made of soft PM (i.e., PZT-5H). The HC cellular networks were assumed to be poled
113 in two directions, i.e., aligned with the pore axis (longitudinally poled (LP) network) and
114 perpendicular to the pore axis (transversely poled (TP) network).

115 **Constitutive Model of Piezoelectric Cellular Material**

116 The linearized constitutive equations for a piezoelectric material are given by:

117
$$\begin{aligned} \varepsilon_{ij} &= S^{E}_{ijkl}\sigma_{kl} + d_{kij}E_k \\ D_i &= d_{ikl}\sigma_{kl} + \kappa^{\sigma}_{ij}E_j \end{aligned} \qquad (1)$$

The ε_{ij}, σ_{ij}, D_i and E_i represent the strain tensor, stress tensor, electric displacement vector, and electric field vector, respectively. The material constants S^E_{ijkl}, κ^σ_{ij}, and d_{ijk} referred to as the fourth-order compliance tensor measured at zero or constant electric field, the second order dielectric tensor measures at zero or constant stress and the components of the piezoelectric strain tensor. Further discussions on the PM constitutive relations can be found elsewhere (Yang 2006). To obtain the homogenized electromechanical properties ($\bar{S}^E_{ijkl}$, $\bar{d}_{kij}$, and $\bar{\kappa}^\sigma_{ij}$) of the UC, Eq. (1) can be written in terms of average stresses $\bar{\sigma}_{ij}$, strains $\bar{\varepsilon}_{ij}$, electric field $\bar{E}_i$, and electric displacement $\bar{D}_i$.

$$\begin{aligned} \bar{\varepsilon}_{ij} &= \bar{S}^E_{ijkl}\bar{\sigma}_{kl} + \bar{d}^E_{kij}\bar{E}_k \\ \bar{D}_i &= \bar{d}^\sigma_{ikl}\bar{\sigma}_{kl} + \bar{\kappa}^\sigma_{ij}\bar{E}_j \end{aligned} \quad (2)$$

According to Eq. (2), the modeling of electromechanical behavior of the cellular PMs requires computing 45 independent material constants, comprising 6 dielectric, 18 piezoelectric and 21 elastic constants.

We considered the linearized electromechanical coupled constitutive relations for each ligament material to obtain the homogenized electromechanical properties of the proposed cellular network. These linearized constitutive relations are simple and, arguably, the most practical method for describing the electromechanical behavior of cellular network at the macroscale (Challagulla and Venkatesh 2013, Iyer et al. 2014, Kar-Gupta and Venkatesh 2006, Sigmund et al. 1998). These assumptions lead to an orthotropic linear electromechanical material model. However, there are advanced models available in the literature (Misra and Poorsolhjouy 2016, Rosi and Auffray 2016, Dell'Isola et al. 2018) that showed that linear microelements in an RVE would produce a nonlinear homogenized response. The geometry-driven non-linearity prevents the use of linear models as

linear models do not correctly exhibit the complexity and inter-connectivity of different parameters involved in formulating the problem. In the present study, we do not consider models that account for geometry-driven nonlinearity. However, it will be interesting to analyze the proposed cellular network using such advanced models that account for higher order gradient theory and geometry-driven non-linearity.

It should be emphasized here that the use of linearized electromechanical coupled constitutive relations has some implications. For example, higher order gradient continuum models have been recently used by several researchers to investigate the dispersive wave propagation in strain gradient elastic media. Contrary to classical elasticity within the strain gradient framework, Rosi and Auffray (Rosi and Auffray 2016) showed that the wave propagation in hexagonal lattices becomes anisotropic and group velocity was proven to be different from energy velocity and should be treated as different quantities. Misra and Poorsolhjouy (Misra and Poorsolhjouy 2016) derived a micro-morphic continuum model for the elasticity of granular media, and the dispersion graphs have presented showing the relationship between the dispersion behavior and the micro-scale parameters. Contrary to classical elasticity, where all the waves will be of an acoustic type, and there will be no possibility of frequency band gaps, the micro-morphic continuum model can show band gaps over a large range of wave numbers. Their results indicate that materials with specific wave propagation behaviors can be designed that can replace existing PMs which are commonly used in damage identification or vibration control applications.

Micromechanical Finite Element Model for Piezoelectric Cellular Materials

Recently, Khan and Abu Al-Rub (Khan and Abu Al-Rub 2017, 2018a; b) developed an FE-based UC homogenization method to predict the overall mechanical properties of periodic architectured materials based on the microstructure geometry and its base material properties. In

this study, we have extended the framework to calculate the overall properties of architected and periodic cellular PMs. Figure 1 shows the UCs of the three types of hexagonal HC structures. Periodic boundary conditions (PBCs) are imposed on UC (Luxner et al. 2005, Kanit et al. 2003; Khan and Muliana 2009, Choudhry et al. 2016) that yield the responses of infinitely repeating patterns of architecture (Jiang et al. 2002, Abueidda et al. 2015). PBCs give quite reasonable estimates of the properties as compared to the homogeneous displacement and homogeneous traction boundary conditions (Zohdi and Wriggers 2005, Xia et al. 2003). Using the proposed framework, it is possible to characterize the linear electromechanical response of piezoelectric architecture materials completely.

Finite Element Models

FE models of the HC based cellular materials were created by varying the ligament orientation ranging from 30-60 degree which corresponds to porosity values ranging from 50-85%. The FE analyses on the UC were performed with the ABAQUS/Standard. A soft piezoelectric material (PZT-5H) was considered as a base material for the cellular material and its electromechanical properties are presented in Table 1. A representative FE model of HC RE is shown in **Figure** 2 with its corresponding 6 boundary faces direction notations. UC has meshed with 10-noded quadratic piezo-electric tetrahedron elements (C3D10E). Each node in C3D10E has a total of four degrees of freedom (DOF), three displacements (u_1, u_2, u_3), and one electrical potential (ϕ). To avoid the rigid body motion of the UC, under electrical loading cases, the locations of arbitrary points A, B, and C that are constrained specifically are also shown in **Figure** 2.

The cellular materials were assumed to be poled longitudinally and transversely. We have assumed that every region of the FE model considered in this study was poled uniformly in one preferred direction. Uniform poling of the piezoelectric HCs normal to transverse porosity

direction is a very challenging task. However, fabrication of the cellular HCs porous networks with uniform poling along the longitudinal direction has been successfully demonstrated (Fey et al. 2016).

Boundary conditions and homogenization for RVE

PBCs are usually applied to the UC to ensure that UC represents the response of the whole architected foam. Moreover, the displacements compatibility and the electric potential continuity across neighboring UC boundaries are assured (Iyer and Venkatesh 2010, Iyer and Venkatesh 2011).

Xia et al. (Xia et al. 2003) developed periodic boundary conditions for a UC in terms of average contractions and stretches ($c_i^j, i = j = 1,2,3$)and shear deformations ($c_i^j, i \neq j$) of the UC model,

$$u_i^{j+}(\mathrm{x},\mathrm{y},\mathrm{z}) - u_i^{j-}(\mathrm{x},\mathrm{y},\mathrm{z}) = c_i^j \qquad (i, j = 1,2,3) \tag{3}$$

The $u_i^{j+}(\mathrm{x},\mathrm{y},\mathrm{z})$ and $u_i^{j-}(\mathrm{x},\mathrm{y},\mathrm{z})$ are the displacements on the positive and negative X_j directions, respectively. Similarly, the PBCs for the electric potential are given by as follows

$$\phi^{j+}(\mathrm{x},\mathrm{y},\mathrm{z}) - \phi^{j-}(\mathrm{x},\mathrm{y},\mathrm{z}) = \bar{E}_i\,(\mathrm{x}_i^{j+} - x_i^{j-}) \qquad (i = 1,2,3) \tag{4}$$

Where, $\bar{E}_i$ is the applied macroscopic electric field. The Eq. (3) and (4) are sufficient to ensure the displacements compatibility and the electric potential continuity.

One of the requirements of the Eq. (3) is that on the two opposite boundary surfaces, the difference of the displacements of the corresponding points should be specified. However, Li (Li 2008) derived an explicit displacement BCs of UCs representing microstructure of periodic structure taken from the symmetry existent within the structure. In this study, the Li (Li 2008) work has been extended to account for electric charge continuity across neighboring UCs and the mixed

boundary conditions are proposed to compute the overall properties of piezoelectric architected materials. Table 2 shows the list of the B.C.s.

To couple micro-macro scale behavior, a homogenization method was adopted to obtain the overall properties of the UC under various global loading conditions. The volume averaging approach was used to compute the average stress and strain as follows:

$$\bar{\sigma}_{ij} = \frac{1}{V}\int_V \sigma_{ij}\left(x,y,z\right)dV \qquad \bar{\varepsilon}_{ij} = \frac{1}{V}\int_V \varepsilon_{ij}\left(x,y,z\right)dV \tag{5}$$

Analogously the average electric fields and electric displacements are defined by

$$\bar{E}_i = \frac{1}{V}\int_V E_i\left(x,y,z\right)dV \qquad \bar{D}_i = \frac{1}{V}\int_V D_i\left(x,y,z\right)dV \tag{6}$$

Considering the traction continuity, the average stress can be written as

$$\bar{\sigma}_{ij} = \frac{R_{ij}}{A_j}\ \left(\text{no summation on j}\right) \tag{7}$$

Using an electric charge continuity, the macroscopic electric displacement is given by

$$\bar{D}_i = \frac{q_i}{A_i} \tag{8}$$

Eq. (7) shows that the macroscopic stress over the UC can be computed from the total tractions (R_{ij}) and the corresponding surfaces areas (A_j). Similarly, Eq. 8 establishes that the macroscopic electrical displacement over the UC can be computed from the total charge (q_i) and the areas (A_i) of the corresponding boundary surfaces.

Sanity Check

In the literature, there is yet no analytical formulation available that offer explicit computation of the properties of the piezoelectric HC networks while their ligaments following orthotropic

material behavior. Hence, the mixed boundary conditions given in Table 2 was applied to one element and 100x100x100 elements cube to evaluate the correctness and appropriateness of the proposed methods. It was found that the proposed approach yields the homogenous properties of the PZT-5H given in Table 1.

Results and Discussion

To compute the effective properties of each unit cells, we applied the appropriate boundary conditions given in **Table** 2. For each load-case, it was ensured that the applied boundary conditions produced only one non-zero component of the macroscopic stress or electric field vector in Eq. (2). Using all set of the B.C.s, the 45 independent material constants could be determined. **Table** 2 shows some of the relations for the calculation of typical material parameters.

The effective properties of each of the three piezoelectric cellular HC network, such as, components of the elastic compliance, $\bar{S}^{E}_{ijkl}$, piezoelectric strain tensors, $(\bar{d}^{E}_{kij}, \bar{d}^{\sigma}_{ikl})$, dielectric stress tensor, $\bar{\kappa}^{\sigma}_{ij}$, and the corresponding elastic constants, $\bar{C}^{E}_{ijkl}$, elastic moduli, $(E^{E}_{ij}, \mathrm{G}^{E}_{kk})$, and Poisson's ratio, were obtained using proposed procedure. For both the LP and TP networks, all material parameters were computed for a wide range of the ligaments' orientation. As the level of auxeticity and UC microstructure are controlled by θ, all the results were shown as a function of varying θ. Since some of the material parameters cannot be directly computed from the FE results, so, the most commonly used material constant of the PMs are derived from the following relations.

$$\begin{gathered}\left[\boldsymbol{C}^{E}\right]=\left[\boldsymbol{S}^{E}\right]^{-1};\ [\boldsymbol{e}]=[\boldsymbol{d}]\left[\boldsymbol{C}^{E}\right];\ \left[\kappa^{\varepsilon}\right]=\left[\kappa^{\sigma}\right]-[\boldsymbol{d}][\boldsymbol{e}]^{T} \\ \left[\boldsymbol{S}^{D}\right]=\left[\boldsymbol{S}^{E}\right]-[\boldsymbol{d}]^{T}[\boldsymbol{g}];\ \left[\boldsymbol{C}^{D}\right]=\left[\boldsymbol{S}^{D}\right]^{-1};\ [\boldsymbol{g}]=[\boldsymbol{h}]\left[\boldsymbol{S}^{D}\right];\ [\boldsymbol{h}]=\left[\kappa^{\varepsilon}\right][\boldsymbol{e}]\end{gathered} \tag{9}$$

Where $\left[\boldsymbol{C}^{D}\right]$ and $\left[\boldsymbol{S}^{D}\right]$ are the components of the stiffness and compliance tensor measured at zero electric displacements, respectively. The $[\boldsymbol{e}]$, $[\boldsymbol{h}]$, $[\boldsymbol{g}]$ are the piezoelectric stress tensor,

strain tensor, and voltage tensor, respectively. The dielectric strain tensor $\left[\kappa^{\varepsilon}\right]$ is computed at zero strain.

Effective Elastic Response

The Compliance matrix coefficients $\bar{S}_{ijkl}^{E}$ were used to calculate the stiffness constants $\bar{C}_{ijkl}^{E}$. **Figure** 3 illustrates the stiffness constants of longitudinally and TP HC structures over various angles 30°, 45°, and 60°. Both LP and TP HC cellular materials showed substantial variations in both in-plane and out-of-plane stiffness coefficients values for different θ. The elastic properties were found to be anisotropic and showed different trends and non-intuitive behavior.

The stiffness constants of the LP and TP HC network (except the in-plane stiffness constants, C_{12}) varied nonlinearly with the increase of the θ. The conventional piezoelectric HCs exhibit considerably superior in-plane stiffness constants C_{12}, C_{13} and C_{22} as compared to the re-entrant and semi re-entrant HC foams, whereas the re-entrant HC foams exhibited significantly improved in-plane stiffness constants such as C_{11}.

For all the HC cellular structures considered, the normal stiffness constants in the longitudinal direction (such as C_{33}) are usually larger than the in-plane stiffness coefficients (such as C_{11} or C_{22}). The high stiffness along the longitudinal direction (3 directions) is a result of stretching dominated mode of deformation while the lower stiffnesses along the in-plane directions (1 or 2 directions) show that the bending dominated deformation behavior. For both poling directions, the highest stiffness was observed for re-entrant HC cellular structures.

However, the out-of-plane normal stiffness constant C_{13} showed higher stiffness as compared to the in-plane stiffness constant C_{12}. The in-plane compliant behavior is due to the fact that the in-plane Poisson's ratio of the HC network is about one order of magnitude higher than the out of

plane Poisson's ratio. For example, the in- (v_{12}) and out-of- (v_{13}) plane Poisson's ratio of the conventional HC with an angle of ligaments of 30^0 is 0.44 and 0.034, respectively.

The shear stiffness constants involving the in-plane shear stiffness constant, C_{44}, and out-of-plane stiffness constant, C_{66}, varied nonlinearly with the increase of the ligament angle (θ). The nonlinear relation between the relative density and ligament angle might be the cause of the nonlinear stiffness behaviors. However, with the increase of θ the out-of-plane shear stiffness constant in, C_{55}, showed a linear trend (Zhang and Ashby 1992). Under the out-of-plane shear loading condition, the deformation behavior along the 3-directions is stretching dominated that makes the HC cellular network stiffer. On the other hand, the in-plane shear stiffness constant, C_{44}, showed a nonlinear trend with the increase of θ. During in-plane shear loading, the ligaments of the HC network deform under bending along the directions 1 and 2. Among the three HC cellular networks, the semi re-entrant HC was observed to have highest in-plane (i.e., C_{44}) and out-of-plane shear stiffness's (i.e., C_{55}, C_{66}) both in longitudinally and transversely porous HC cellular materials. In addition, for the proposed HC cellular networks a diverse range of in-plane ν can be obtained (+ve, -ve and zero). **Figure** 5 shows that the biggest positive +ve and -ve in-plane ν's were observed at an angle of 30^0. **Figure** 4 and 5 results demonstrate that the HC based piezoelectric cellular materials can yield unique sets of elastic properties with different level of auxeticity.

Figure 6 shows the displacement and electric potential contour plots for three different load case. For all three HC structures considered, the displacement contours in 1-direction under uniaxial and shear loading loadings are shown in **Figures** 6(a) and (b), respectively. These distributions of displacement fields clearly demonstrated the state of shear and uniaxial deformation behavior. For the loading case-7, the electric field of 0.1MV/m is applied, and the electric potential contours

plots are obtained. **Figure** 6(c) shows that for all three HC network, there is a linear variation of electrical potential between opposite faces of loading while a uniform electric potential was observed at the central part of the UCs.

Effective piezoelectric properties

Figure 7 shows the changes in the overall piezoelectric properties as a function of the angle of ligaments for HC cellular networks considered. The poling direction with respect to the porosity axis usually has an insignificant effect on the piezoelectric properties of porous materials (Iyer et al. 2015). However, it is observed for both TP and LP HC networks that the architecture of the HC cellular network does affect some of the piezoelectric properties. The level of magnitude of piezoelectric properties of TP networks are very less as compared to the LP HC network, but variation response as a function of ligament angle has similar trends.

We analyzed both the normal and shear piezoelectric coefficients. It was found that shear piezoelectric properties of HC cellular network exhibited high piezoelectric sensitivity. However, the shear piezoelectric constants showed considerably different behavior as a function of θ. In the case of LP HC network, the e_{24} (LP) was increased, and e_{15} (LP) was decreased significantly with θ for all HC networks. The largest value of e_{15} (LP) was observed at 30 degrees for a re-entrant network; while for e_{24} (LP) the semi-re-entrant HC network was showing the highest values and increased with the values of θ.

The effective normal piezoelectric properties were found to be a function of ligament angle and HC networks architecture. The normal piezoelectric constant, $e_{33,}$ is usually recognized as the most vital parameter for various applications utilizing monolithic PMs. For LP HC network e_{33} (LP) was amplified with the increase in ligament angle, but there was an insignificant variation for e33(TP). In addition, **Figure** 7 demonstrated that even though the e31 of the ligament base material has

negative values, the HC network could display both -ve and +ve values of e_{31} values by varying the angle θ. These results indicated that the piezoelectric HC architecture could show a different crystal symmetry as compared to the ligament base material. The LP HC network produced the highest negative values of e_{31} and e_{32}.

Effective dielectric properties

The effective dielectric constants κ_{ij} were computed for all three HC cellular networks as a function of the θ as presented in **Figure** 8. Both LP and TP HC cellular networks showed noteworthy variations in the κ_{ij} values at various angles. The κ_{ij} values of all piezoelectric HC networks (except $\kappa_{11}(\mathrm{LP})$ and $\kappa_{11}(\mathrm{TP})$ for conventional and semi re-entrant HC) increased and varied nonlinearly as a function of ligaments angle. The decrease in the magnitudes of $\kappa_{11}(\mathrm{LP})$ and $\kappa_{11}(\mathrm{TP})$ for conventional and semi re-entrant HC was related to the scattered path of the electric charges along the x-axis. The highest and lowest values of the κ_{ij} were obtained for re-entrant HC $\kappa_{33}(\mathrm{LP})$ and conventional HC, $\kappa_{11}(\mathrm{TP})$, respectively.

Effective Figure of Merit

Various figures of merit (FOM) are of interest to evaluate the usefulness of PMs in industrial applications, such as an ultrasound imager, hydrophones, and energy harvesters. The combination of fundamental electromechanical coefficients (i.e., elastic, piezoelectric and dielectric coefficients as calculated by the above mentioned FEA) can be used to evaluate numerous industrial FOM. For cellular network FOM, the relevant constants in various applications (i.e., hydrophones) are the hydrostatic strain coefficient (d_h), the hydrostatic FOM ($d_h.\mathrm{g}_h$), the acoustic impedance (Z) and electromechanical thickness model coupling factor (k_t) (Kar-Gupta and Venkatesh 2006, Dunn and Taya 1993b). There are some other FOM which are of importance in several different

applications. The relevant FOM parameters are given in Table 3. More details on FOMs can be found elsewhere, (Dunn and Taya 1993b).

To assess how much the proposed HC networks enhanced the electromechanical responses the FOM of the HC network is normalized with the FOM of monolithic PM (PZT-5H) as shown in **Figure** 8. For the TP networks, the results show that all the normalized FOMs did not show any enrichment in electromechanical behavior. However, in the LP networks, some of the normalized FOMs varied strongly and marginally as a function of θ. The normalized d_h showed a very minor effect on the variation of θ while a normalized $d_h.g_h$ was decreased with the increase in the θ and the highest value was found at 30 degrees. The inverse relation between g_{33} and κ_{33} is the cause of such huge improvement in the $d_h.g_h$. **Figure** 8 shows that the κ_{ij} decreases with the increase of porosity, and as a result, the g_h was increased. The lowest (better) normalized value of Z was found at 30^0 while the Z value increases with an increase in the θ. The numerical results agreed well with the experimentally observed (Bast and Wersing 1989) trend of decrease in the values of Z with the increase of porosity.

The proposed piezoelectric HC cellular material showed an improved behavior for the LP system as compared to the bulk material. For example, the LP HC networks showed one order of magnitude increase in their hydrostatic FOM. However, the acoustic impedance was decreased by one order of magnitude.

The Z-$d_h.g_h$ relationship is important to be analyzed while designing the transducer and hydrophones. **Figure** 9 shows the Z-$d_h.g_h$ quid pro quo, where when the porosity of HC networks increases, the $d_h.g_h$ showed increasing trend while the Z value decreases. Such a quite unique combination of increased sensitivity and reduced acoustic impedances is nearly impossible to

obtain using bulk PMs and piezoelectric composites (Dunn and Taya 1993a). These results indicate that it is possible to design architected porous PM with required electromechanical characteristics. Several researchers have shown that auxetic geometry improves the performance of the piezoelectric composite and porous PMs. For piezoelectric composites, Smith (Smith 1991) showed that the polymer matrix with negative Poisson's ratio enhances their performance. Numerous studies combined topology optimization and finite element methods to design optimum topologies of unit cells to obtain a piezoelectric composite with better behavior. Using the topology optimization method proposed by Bendsøe and Kikuchi (Bendsøe and Kikuchi 1988), the optimum design of 1-3 piezoelectric composites for hydrophone applications were obtained by Sigmund et al (Sigmund et al. 1998). Using the criteria to maximize for d_h and $d_h.g_h$, the obtained optimal 3D porous architected matrix showed auxetic effects in certain directions like re-entrant type HC cellular material. Moreover, the optimized design with porous architecture design increases the values of d_h and $d_h.g_h$ over monolithic piezoelectric ceramics by factors of more than 10 and 10,000, respectively. A unit cell based topology optimization approach was proposed by Silva, Kikuchi, and co-workers (Silva et al. 1997, Silva et al. 1998) to find the distribution of inclusion and/or voids phases that enhances piezoelectric electromechanical efficiency. Several 2D and 3D auxetic structures (negative Poisson's ratio) consisting of piezoelectric polymer and architected cellular materials were proposed.

For the proposed piezoelectric HC cellular networks, a desirable elastic, piezoelectric and dielectric properties can be obtained that is nearly impossible to achieve using bulk PMs and piezoelectric composites. The unique set of electromechanical properties is a function of angle so all the properties cannot be improved at once. It requires some techniques to obtain an optimum combination of properties. For example, using topology optimization Sigmund et al. (Sigmund et

al. 1998) showed that the cell design should be optimized such that it gives the required strength and electromechanical properties. The proposed 3-1 type piezoelectric cellular networks are limited in terms of their electromechanical properties and strength. Recently, we have shown that 3-3 type piezoelectric metamaterials can provide a good combination of strength and electromechanical properties (Khan and Khan 2019). The 3-3 type piezoelectric porous metamaterials design improves the values of d_h and $d_h.g_h$ over monolithic piezoelectric ceramics by factors of more than 15 and 12,000, respectively.

Next, we analyzed the behavior of normalized electromechanical coupling factors (k_{31}, k_{32}, k_t) and frequency constants (N_{31}, N_{32}, N_t).**Figures** 10(a-c) showed the normalized magnitudes of the k_{3i} and k_t . The k_{31} decreased while k_{32} increased with the increase in angle θ. The k_{31} and k_{32} were equal for the bulk PZT-5H. For all proposed HC cellular materials, for given angles, the k_{31} values ware seen to decrease more comparative to k_{32} because of the anisotropic nature of microstructure. For both modes, the d_{3i} were nearly equal but the higher values of S_{11}^E than S_{22}^E give rise to more decrease in k_{31} than k_{32}. In contrast, to k_{31} and k_{32}, the normalized kt values were one order higher than the monolithic PZT-5H.

Figures 9(d-f) showed normalized plots of N_1 and N_2. For monolithic material, the frequency constants N_1 and N_2 were equal. For all the proposed HC cellular materials, for given angles, the N_1 values were seen to decrease more comparative to N_2. As compared to monolithic piezoelectric materials, the disparity in N_1 and N_2 values were due to the orthotropic constituent properties and the architecture of the HC cellular materials. Moreover, the reverse trend was observed for N_1 and N_2 with an increase in the porosity. The larger decreased in N_1 than N_2 values are due to the higher values of S_{11}^E than S_{22}^E . The normalized Nt decreased with the increase of porosity as shown in

406 **Figure** 10(f). The decreased in N_t with increasing the porosity was linked with the increased in the
407 S_{33}^{E} due to decrease in the transverse damping.

408 The computational analyses show that the relationship between the architecture of HC cellular
409 network and anisotropic nature of constituent properties leads to architecture-dependent elastic,
410 piezoelectric and dielectric properties that vary significantly from the properties of the monolithic
411 material. Among all three proposed HC networks, the CHC cellular materials showed exceptional
412 electromechanical properties. The FE results confirm that the RE and SRE HC network
413 demonstrate a combination of unique mechanical properties with auxetic effects and exceptional
414 piezoelectric properties which cannot be realized from CHC network. Overall, the FE results
415 endorsed that the cellular networks can be tailored to obtain a unique combination of tunable
416 electromechanical properties as per the needs of various practical applications. The proposed novel
417 RE and SRE HC networks have the capacity to design unique next generation actuators and sensors
418 with negative and zero Poisson's ratio.

419 **Conclusions**

420 This study proposed a finite element base micromechanical modeling framework to estimate
421 the elastic, dielectric and piezoelectric of the HC based cellular PMs. Using the internal symmetry
422 of the periodic structure a mixed boundary conditions analogous to PBCs were proposed. The
423 modeling approach was applied to the UCs of conventional, auxetic and semi re-entrant type HC
424 piezoelectric cellular networks and their electromechanical properties were presented. For the
425 longitudinal poled network, the results showed that the HC network exhibited an exceptional
426 combination of piezoelectric properties, i.e., low impedance and more sensitivity, which could not
427 be obtained by monolithic PMs. However, for the TP network, the electromechanical properties
428 displayed insignificant dependence on the porosity and angle of the ligament. The FE results

showed that HC network with tunable electromechanical characteristics coupled with auxetic behavior such as negative or zero Poisson's ratio could be produced. Such novel HC network-based functional cellular materials have the capacity to facilitate the design of light-weight devices for various next-generation sensors and actuators.

ACKNOWLEDEMENTS

The authors would like to thank undergraduate students Abdelrahman Alhammadi, Ali Alneyadi and Saeed Alqaydi from Khalifa University of Science and Technology for generating CAD files of the HC cellular networks.

REFERENCES

Abueidda, D. W., Dalaq, A. S., Abu Al-Rub, R. K., and Younes, H. A. (2015). "Finite element predictions of effective multifunctional properties of interpenetrating phase composites with novel triply periodic solid shell architectured reinforcements." *International Journal of Mechanical Sciences*, 92, 80–89.

Alkhader, M., Iyer, S., Shi, W., and Venkatesh, T. A. (2015). "Low frequency acoustic characteristics of periodic honeycomb cellular cores: The effect of relative density and strain fields." *Composite Structures*, 133, 77–84.

Alkhader, M., and Vural, M. (2009). "The partition of elastic strain energy in solid foams and lattice structures." *Acta Materialia*, 57(8), 2429–2439.

Banno, H. (1985). "Theoretical equations for dielectric and piezoelectric properties of ferroelectric composites based on modified cubes model." *Japanese Journal of Applied Physics*, 24(S2), 445.

Bast, U., and Wersing, W. (1989). "The influence of internal voids with 3–1 connectivity on the properties of piezoelectric ceramics prepared by a new planar process." *Ferroelectrics*, 94(1), 229–242.

Bauer, J., Hengsbach, S., Tesari, I., Schwaiger, R., and Kraft, O. (2014). "High-strength cellular ceramic composites with 3D microarchitecture." *Proceedings of the National Academy of Sciences*, 111(7), 2453–2458.

Bendsøe, M. P., and Kikuchi, N. (1988). "Generating optimal topologies in structural design using a homogenization method." *Computer methods in applied mechanics and engineering*, 71(2), 197–224.

Bosse, P. W., Challagulla, K. S., and Venkatesh, T. A. (2012). "Effects of foam shape and porosity aspect ratio on the electromechanical properties of 3-3 piezoelectric foams." *Acta Materialia*, 60(19), 6464–6475.

Bowen, C. R., Perry, A., Lewis, A. C. F., and Kara, H. (2004). "Processing and properties of porous piezoelectric materials with high hydrostatic figures of merit." *Journal of the European Ceramic Society*, 24(2), 541–545.

Bowen, C. R., and Topolov, V. Y. (2003). "Piezoelectric sensitivity of PbTiO 3-based ceramic/polymer composites with 0–3 and 3–3 connectivity." *Acta materialia*, 51(17), 4965–4976.

Challagulla, K. S., and Venkatesh, T. A. (2012). "Electromechanical response of piezoelectric foams." *Acta Materialia*, 60(5), 2111–2127.

Challagulla, K. S., and Venkatesh, T. A. (2013). "Computational Modeling of Piezoelectric Foams." *JOM*, 65(2), 256–266.

Choudhry, R. S., Khan, K. A., Khan, S. Z., Khan, M. A., and Hasan, A. (2016). "Micromechanical Modeling of 8-Harness Satin Weave Glass Fiber Reinforced Composites." *Journal of Composite Materials*.

Dell'Isola, F., Seppecher, P., Alibert, J. J., Lekszycki, T., Grygoruk, R., Pawlikowski, M., Steigmann, D., Giorgio, I., Andreaus, U., and Turco, E. (2018). "Pantographic metamaterials: an example of mathematically driven design and of its technological challenges." *Continuum Mechanics and Thermodynamics*, 1–34.

Dunn, M. L., and Taya, M. (1993a). "Micromechanics predictions of the effective electroelastic moduli of piezoelectric composites." *International Journal of Solids and Structures*, 30(2), 161–175.

Dunn, M. L., and Taya, M. (1993b). "Electromechanical Properties of Porous Piezoelectric Ceramics." *Journal of the American Ceramic Society*, 76(7), 1697–1706.

Elhajjar, R., La Saponara, V., Muliana, A., Lin, Y., and Sodano, H. A. (2013). "Active Fiber Composites." *Smart Composites: Mechanics and Design*, CRC Press, 99–128.

Fang, P., Wegener, M., Wirges, W., Gerhard, R., and Zirkel, L. (2007). "Cellular polyethylene-naphthalate ferroelectrets: Foaming in supercritical carbon dioxide, structural and electrical preparation, and resulting piezoelectricity." *Applied physics letters*, 90(19), 192908.

Fey, T., Eichhorn, F., Han, G., Ebert, K., Wegener, M., Roosen, A., Ken-ichi Kakimoto, and Greil, P. (2016). "Mechanical and electrical strain response of a piezoelectric auxetic PZT lattice structure." *Smart Materials and Structures*, 25(1), 015017.

Geis, S., Löbmann, P., Seifert, S., and Fricke, J. (2000). "Dielectric properties of PZT aerogels." *Ferroelectrics*, 241(1), 75–82.

Gibson, L. J., and Ashby, M. F. (1997). *Cellular solids: structure and properties*. Cambridge university press.

Grima, J. N., Oliveri, L., Attard, D., Ellul, B., Gatt, R., Cicala, G., and Recca, G. (2010). "Hexagonal honeycombs with zero Poisson's ratios and enhanced stiffness." *Advanced Engineering Materials*, 12(9), 855–862.

Hikita, K., Yamada, K., Nishioka, M., and Ono, M. (1983). "Piezoelectric properties of the porous PZT and the porous PZT composite with silicone rubber." *Ferroelectrics*, 49(1), 265–272.

Iyer, S., Alkhader, M., and Venkatesh, T. A. (2014). "Electromechanical response of piezoelectric honeycomb foam structures." *Journal of the American Ceramic Society*, 97(3), 826–834.

Iyer, S., Alkhader, M., and Venkatesh, T. A. (2015). "Electromechanical behavior of auxetic piezoelectric cellular solids." *Scripta Materialia*, 99, 65–68.

Iyer, S., and Venkatesh, T. A. (2010). "Electromechanical response of porous piezoelectric materials: Effects of porosity connectivity." *Applied Physics Letters*, 97(7), 072904.

Iyer, S., and Venkatesh, T. A. (2011). "Electromechanical response of (3-0) porous piezoelectric materials: Effects of porosity shape." *Journal of Applied Physics*, 110(3), 034109.

Jiang, M., Jasiuk, I., and Ostoja-Starzewski, M. (2002). "Apparent thermal conductivity of periodic two-dimensional composites." *Computational Materials Science*, 25(3), 329–338.

Kanit, T., Forest, S., Galliet, I., Mounoury, V., and Jeulin, D. (2003). "Determination of the size of the representative volume element for random composites: statistical and numerical approach." *International Journal of solids and structures*, 40(13), 3647–3679.

Kara, H., Ramesh, R., Stevens, R., and Bowen, C. R. (2003). "Porous PZT ceramics for receiving transducers." *Ultrasonics, Ferroelectrics, and Frequency Control, IEEE Transactions on*, 50(3), 289–296.

Kar-Gupta, R., and Venkatesh, T. A. (2006). "Electromechanical response of porous piezoelectric materials." *Acta Materialia*, 54(15), 4063–4078.

Kar-Gupta, R., and Venkatesh, T. A. (2008). "Electromechanical response of piezoelectric composites: Effects of geometric connectivity and grain size." *Acta Materialia*, 56(15), 3810–3823.

Khan, K. A., and Abu Al-Rub, R. K. (2017). "Time dependent response of architectured Neovius foams." *International Journal of Mechanical Sciences*, 126, 106–119.

Khan, K. A., and Abu Al-Rub, R. K. (2018a). "Modeling time and frequency domain viscoelastic behavior of architectured foams." *J. Eng. Mech*, 144(6), 1–15.

Khan, K. A., and Abu Al-Rub, R. K. (2018b). "Viscoelastic properties of architected foams based on the Schoen IWP triply periodic minimal surface." *Mechanics of Advanced Materials and Structures*, 1–14.

Khan, K. A., and Khan, M. A. (2019). "3-3 piezoelectric metamaterial with negative and zero Poisson's ratio for hydrophones applications." *Materials Research Bulletin*, 112, 194–204.

Khan, K. A., and Muliana, A. H. (2009). "A multi-scale model for coupled heat conduction and deformations of viscoelastic functionally graded materials." *Composites Part B: Engineering*, Blast/impact on engineered (nano)composite materials, 40(6), 511–521.

Lee, S.-H., Jun, S.-H., Kim, H.-E., and Koh, Y.-H. (2007). "Fabrication of Porous PZT–PZN Piezoelectric Ceramics With High Hydrostatic Figure of Merits Using Camphene-Based Freeze Casting." *Journal of the American Ceramic Society*, 90(9), 2807–2813.

Lethiecq, M., Levassort, F., and Tran-Huu-Hue, L. P. (2004). "New low acoustic impedance piezoelectric material for broadband transducer applications." *2004 IEEE Ultrasonics Symposium*, 1153-1156 Vol.2.

Levassort, F., Lethiecq, M., Millar, C., and Pourcelot, L. (1998). "Modeling of highly loaded 0-3 piezoelectric composites using a matrix method." *Ultrasonics, Ferroelectrics, and Frequency Control, IEEE Transactions on*, 45(6), 1497–1505.

Li, S. (2008). "Boundary conditions for unit cells from periodic microstructures and their implications." *Composites Science and Technology*, 68(9), 1962–1974.

Luxner, M. H., Stampfl, J., and Pettermann, H. E. (2005). "Finite element modeling concepts and linear analyses of 3D regular open cell structures." *Journal of Materials Science*, 40(22), 5859–5866.

Marselli, S., Pavia, V., Galassi, C., Roncari, E., Craciun, F., and Guidarelli, G. (1999). "Porous piezoelectric ceramic hydrophone." *The Journal of the Acoustical Society of America*, 106(2), 733.

556 Masters, I. G., and Evans, K. E. (1996). “Models for the elastic deformation of honeycombs.”
557 *Composite structures*, 35(4), 403–422.
558 Mikata, Y. (2001). “Explicit determination of piezoelectric Eshelby tensors for a spheroidal
559 inclusion.” *International Journal of Solids and Structures*, 38(40–41), 7045–7063.
560 Misra, A., and Poorsolhjouy, P. (2016). “Granular micromechanics based micromorphic model
561 predicts frequency band gaps.” *Continuum Mechanics and Thermodynamics*, 28(1–2),
562 215–234.
563 Muliana, A. (2011). “Time dependent behavior of ferroelectric materials undergoing changes in
564 their material properties with electric field and temperature.” *International Journal of*
565 *Solids and Structures*, 48(19), 2718–2731.
566 Nagata, K., Igarashi, H., Okazaki, K., and Bradt, R. C. (1980). “Properties of an Interconnected
567 Porous Pb(Zr, Ti)O 3 Ceramic.” *Japanese Journal of Applied Physics*, 19(1), L37–L40.
568 Newnham, R. E., Skinner, D. P., and Cross, L. E. (1978). “Connectivity and piezoelectric-
569 pyroelectric composites.” *Materials Research Bulletin*, 13(5), 525–536.
570 Papka, S. D., and Kyriakides, S. (1999). “Biaxial crushing of honeycombs:—Part 1:
571 Experiments.” *International Journal of Solids and Structures*, 36(29), 4367–4396.
572 Piazza, D., Capiani, C., and Galassi, C. (2005). “Piezoceramic material with anisotropic graded
573 porosity.” *Journal of the European Ceramic Society*, 25(12), 3075–3078.
574 Ramesh, R., Prasad, C. D., Kumar, T. K. V., Gavane, L. A., and Vishnubhatla, R. M. R. (2006).
575 “Experimental and finite element modelling studies on single-layer and multi-layer 1–3
576 piezocomposite transducers.” *Ultrasonics*, 44(4), 341–349.
577 Richard, C., Lee, H. S., and Guyomar, D. (2004). “Thermo-mechanical stress effect on 1-3
578 piezocomposite power transducer performance.” *Ultrasonics*, 42(1–9), 417–424.
579 Rosi, G., and Auffray, N. (2016). “Anisotropic and dispersive wave propagation within strain-
580 gradient framework.” *Wave Motion*, 63, 120–134.
581 Sigmund, O., Torquato, S., and Aksay, I. A. (1998). “On the design of 1–3 piezocomposites
582 using topology optimization.” *Journal of materials research*, 13(4), 1038–1048.
583 Silva, E. C. N., Fonseca, J. S. O., and Kikuchi, N. (1998). “Optimal design of periodic
584 piezocomposites.” *Computer Methods in Applied Mechanics and Engineering*, 159(1–2),
585 49–77.
586 Silva, E. N., Fonseca, J. O., and Kikuchi, N. (1997). “Optimal design of piezoelectric
587 microstructures.” *Computational mechanics*, 19(5), 397–410.
588 Skinner, D. P., Newnham, R. E., and Cross, L. E. (1978). “Flexible composite transducers.”
589 *Materials Research Bulletin*, 13(6), 599–607.
590 Smith, W. A. (1989). “The role of piezocomposites in ultrasonic transducers.” *Ultrasonics*
591 *Symposium, 1989. Proceedings., IEEE 1989*, IEEE, 755–766.
592 Smith, W. A. (1991). “Optimizing electromechanical coupling in piezocomposites using
593 polymers with negative Poisson’s ratio.” *IEEE 1991 Ultrasonics Symposium*, 661–666
594 vol.1.
595 Ting, R. Y. (1985). “Piezoelectric properties of a porous PZT ceramic.” *Ferroelectrics*, 65(1),
596 11–20.
597 Topolov, V. Y., and Bowen, C. R. (2008). *Electromechanical properties in composites based on*
598 *ferroelectrics*. Springer Science & Business Media.
599 Ueda, J., Secord, T. W., and Asada, H. H. (2010). “Large effective-strain piezoelectric actuators
600 using nested cellular architecture with exponential strain amplification mechanisms.”
601 *IEEE/ASME Transactions on Mechatronics*, 15(5), 770–782.

Wadley, H. N. (2006). “Multifunctional periodic cellular metals.” *Philosophical Transactions of the Royal Society of London A: Mathematical, Physical and Engineering Sciences*, 364(1838), 31–68.

Wirges, W., Wegener, M., Voronina, O., Zirkel, L., and Gerhard-Multhaupt, R. (2007). “Optimized Preparation of Elastically Soft, Highly Piezoelectric, Cellular Ferroelectrets from Nonvoided Poly(ethylene Terephthalate) Films.” *Advanced Functional Materials*, 17(2), 324–329.

Xia, Z., Zhang, Y., and Ellyin, F. (2003). “A unified periodical boundary conditions for representative volume elements of composites and applications.” *International Journal of Solids and Structures*, 40(8), 1907–1921.

Yang, J. (2006). *An Introduction to the Theory of Piezoelectricity*. Springer Science & Business Media.

Zhang, H. L., Li, J.-F., and Zhang, B.-P. (2007). “Microstructure and electrical properties of porous PZT ceramics derived from different pore-forming agents.” *Acta Materialia*, 55(1), 171–181.

Zhang, J., and Ashby, M. F. (1992). “The out-of-plane properties of honeycombs.” *International Journal of Mechanical Sciences*, 34(6), 475–489.

Zhu, H. X., Knott, J. F., and Mills, N. J. (1997). “Analysis of the elastic properties of open-cell foams with tetrakaidecahedral cells.” *Journal of the Mechanics and Physics of Solids*, 45(3), 319–343.

Zohdi, T. I., and Wriggers, P. (Eds.). (2005). *An Introduction to Computational Micromechanics*. Lecture Notes in Applied and Computational Mechanics, Springer Berlin Heidelberg, Berlin, Heidelberg.

Table Click here to access/download;Table;4-Tables-Text.docx

Table 1. Electromechanical properties of the PZT-5H (poled in 3-direction)

Properties	PZT-5H
$S_{11}^E = S_{22}^E$ (pm^2 / N)	16.5
$S_{12}^E = S_{21}^E$ (pm^2 / N)	-4.78
$S_{13}^E = S_{23}^E$ (pm^2 / N)	-8.45
S_{33}^E (pm^2 / N)	20.7
S_{44}^E (pm^2 / N)	42.6
$S_{55}^E = S_{66}^E$ (pm^2 / N)	43.5
$d_{15} = d_{24}$ (p m/ V)	741
$d_{31} = d_{32}$ (p m/ V)	-274
d_{33} (p m/ V)	593
$\kappa_{11}^\sigma / \kappa_0 = \kappa_{22}^\sigma / \kappa_0$	3130
$\kappa_{33}^\sigma / \kappa_0$	3400
Density (ρ)	7500 kg/m^3
Permittivity of free space (κ_0)	8.85x10^{-12} C/Vm

Table 2. Complete set of boundary conditions with computation formulae to determine electromechanical coefficients.

Coefficients	X⁻	X⁺	Y⁻	Y⁺	Z⁻	Z⁺	Relation
	$\bar{u}_i / \bar{\phi}$	$\bar{u}_i / \bar{\phi}$	$\bar{u}_i / \bar{\phi}$	$\bar{u}_i / \bar{\phi}$	$\bar{u}_i / \bar{\phi}$	$\bar{u}_i / \bar{\phi}$	
$\bar{S}^E_{11}, \bar{S}^E_{12}$ $\bar{S}^E_{13}, \bar{d}^E_{31}$	0 / 0	$\bar{u}_1$ / 0	0 / 0	– / 0	0 / 0	– / 0	$\bar{\varepsilon}_{11}/\bar{\sigma}_{11}, \bar{\varepsilon}_{22}/\bar{\sigma}_{11}$, $\bar{\varepsilon}_{33}/\bar{\sigma}_{11}, \bar{D}_3/\bar{\sigma}_{11}$
$\bar{S}^E_{21}, \bar{S}^E_{22}$ $\bar{S}^E_{23}, \bar{d}^E_{32}$	0 / 0	– / 0	0 / 0	$\bar{u}_2$ / 0	0 / 0	– / 0	$\bar{\varepsilon}_{11}/\bar{\sigma}_{22}, \bar{\varepsilon}_{22}/\bar{\sigma}_{22}$, $\bar{\varepsilon}_{33}/\bar{\sigma}_{22}, \bar{D}_3/\bar{\sigma}_{22}$
$\bar{S}^E_{31}, \bar{S}^E_{32}$ $\bar{S}^E_{33}, \bar{d}^E_{33}$	0 / 0	– / 0	0 / 0	– / 0	0 / 0	$\bar{u}_3$ / 0	$\bar{\varepsilon}_{11}/\bar{\sigma}_{33}, \bar{\varepsilon}_{22}/\bar{\sigma}_{33}$, $\bar{\varepsilon}_{33}/\bar{\sigma}_{33}, \bar{D}_3/\bar{\sigma}_{33}$
$\bar{S}^E_{44}, \bar{d}^E_{24}$	$\bar{u}_2 = 0$, $\bar{u}_3 = 0$ /0	$\bar{u}_2 = 0$, $\bar{u}_3 = 0$ /0	$\bar{u}_1 = 0$, $\bar{u}_3 = 0$ /0	$\bar{u}_1 \neq 0$, $\bar{u}_3 = 0$ /0	$\bar{u}_3 = 0$ /0	$\bar{u}_3 = 0$ /0	$\bar{\varepsilon}_{12}/\bar{\sigma}_{12}$, $\bar{D}_2/\bar{\sigma}_{12}$
$\bar{S}^E_{55}, \bar{d}^E_{15}$	$\bar{u}_2 = 0$, $\bar{u}_3 = 0$ /0	$\bar{u}_2 = 0$, $\bar{u}_3 = 0$ /0	$\bar{u}_2 = 0$, /0	$\bar{u}_2 = 0$, /0	$\bar{u}_1 = 0$, $\bar{u}_2 = 0$ /0	$\bar{u}_1 \neq 0$, $\bar{u}_2 = 0$ /0	$\bar{\varepsilon}_{13}/\bar{\sigma}_{13}$, $\bar{D}_1/\bar{\sigma}_{13}$
$\bar{S}^E_{66}$	$\bar{u}_1 = 0$, /0	$\bar{u}_1 = 0$, /0	$\bar{u}_1 = 0$, $\bar{u}_3 = 0$ /0	$\bar{u}_1 = 0$, $\bar{u}_3 = 0$ /0	$\bar{u}_1 = 0$, $\bar{u}_2 = 0$ /0	$\bar{u}_1 = 0$, $\bar{u}_2 \neq 0$ /0	$\bar{\varepsilon}_{23}/\bar{\sigma}_{23}$
$\bar{d}^\sigma_{15}, \bar{\kappa}^\sigma_{11}$	* / 0	– / $\bar{\phi}$	– / –	– / –	– / –	– / –	$\bar{\varepsilon}_{13}/\bar{E}_1$, $\bar{D}_1/\bar{E}_1$
$\bar{d}^\sigma_{24}, \bar{\kappa}^\sigma_{22}$	– / –	– / –	* / 0	– / $\bar{\phi}$	– / –	– / –	$\bar{\varepsilon}_{12}/\bar{E}_2$, $\bar{D}_2/\bar{E}_2$
$\bar{d}^\sigma_{31}, \bar{d}^\sigma_{32}$, $\bar{d}^\sigma_{33}, \bar{\kappa}^\sigma_{33}$	– / –	– / –	– / –	– / –	* / 0	– / $\bar{\phi}$	$\bar{\varepsilon}_1/\bar{E}_3, \bar{\varepsilon}_2/\bar{E}_3$ $\bar{\varepsilon}_3/\bar{E}_3, \bar{D}_3/\bar{E}_3$

*Points A, B and C are constrained on respective faces (having zero electric potential) to avoid rigid body motion.

Table 3. List of figure of merit.

Parameter	Relation
hydrostatic strain coefficient (d_h)	$d_h = d_{31} + d_{32} + d_{33}$
hydrostatic figure of merit ($d_h.g_h$)	$g_h d_h$ with $g_h = g_{31} + g_{32} + g_{33}$
acoustic impedance (Z)	$Z = \left[\rho C_{33}^E \right]^{1/2}$
electromechanical thickness mode coupling factor (k_t)	$k_t = \left[1 - \frac{C_{33}^E}{C_{33}^D} \right]^{1/2} = \frac{e_{33}}{\left[C_{33}^D \kappa_{33}^{\varepsilon} \right]^{1/2}}$
electromechanical coupling factor (k_{3i})	$k_{3i} = \frac{d_{3i}}{\left[S_{ii}^E \kappa_{33}^{\sigma} \right]^{1/2}}$; (i=1,2 with no sum on ii)
Frequency constants(N_t)	$N_t = \frac{1}{2}\left[\frac{C_{33}^E}{\rho} \right]^{1/2}$
Frequency constants(N_i)	$N_i = \frac{1}{2}\left[\frac{1}{\rho S_{33}^E} \right]^{1/2}$; (i=1,2 with no sum on ii)

Figure

Click here to access/download;Figure;Figure1.tiff

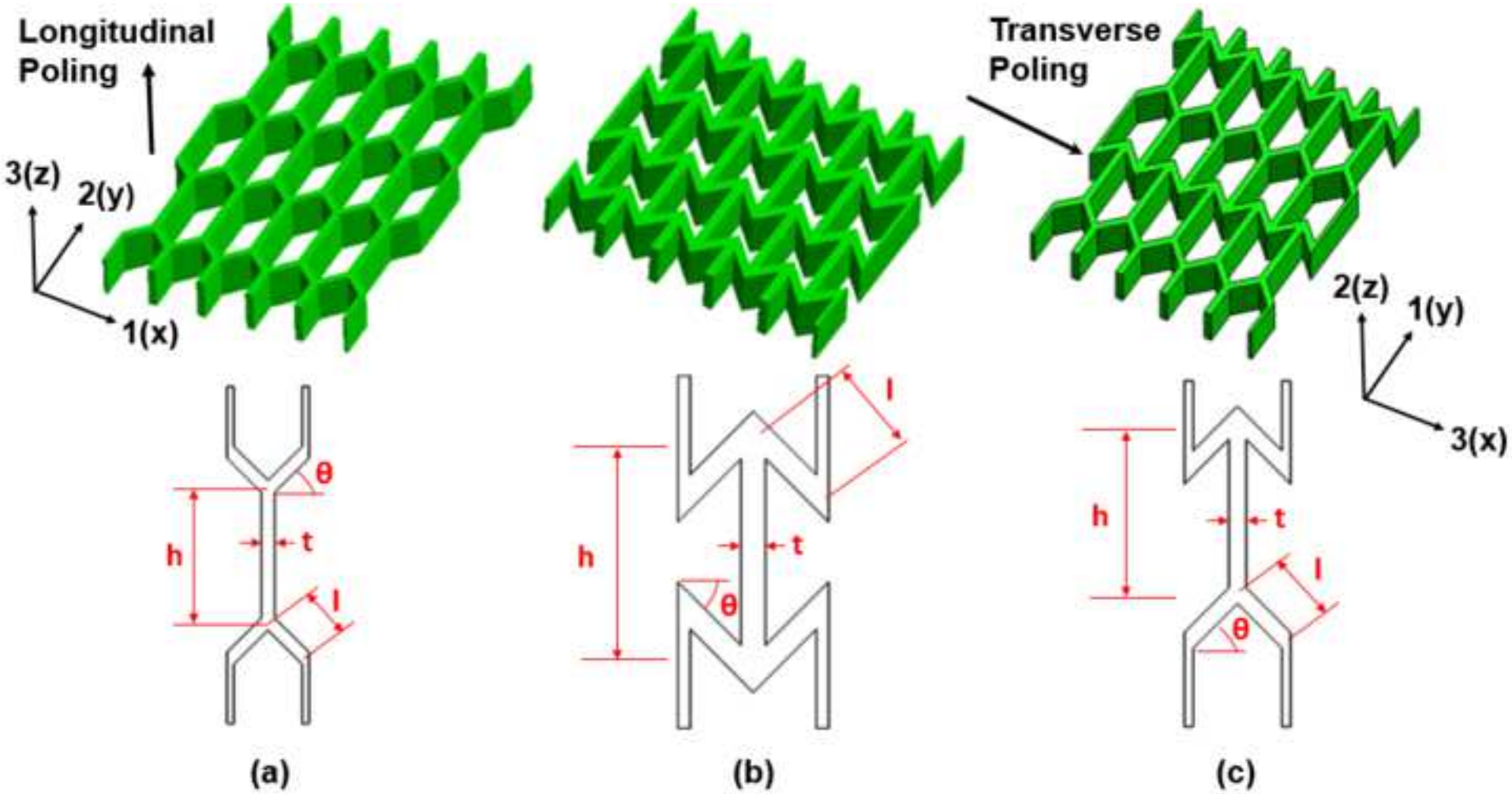

Figure

Click here to access/download;Figure;Figure2.tiff

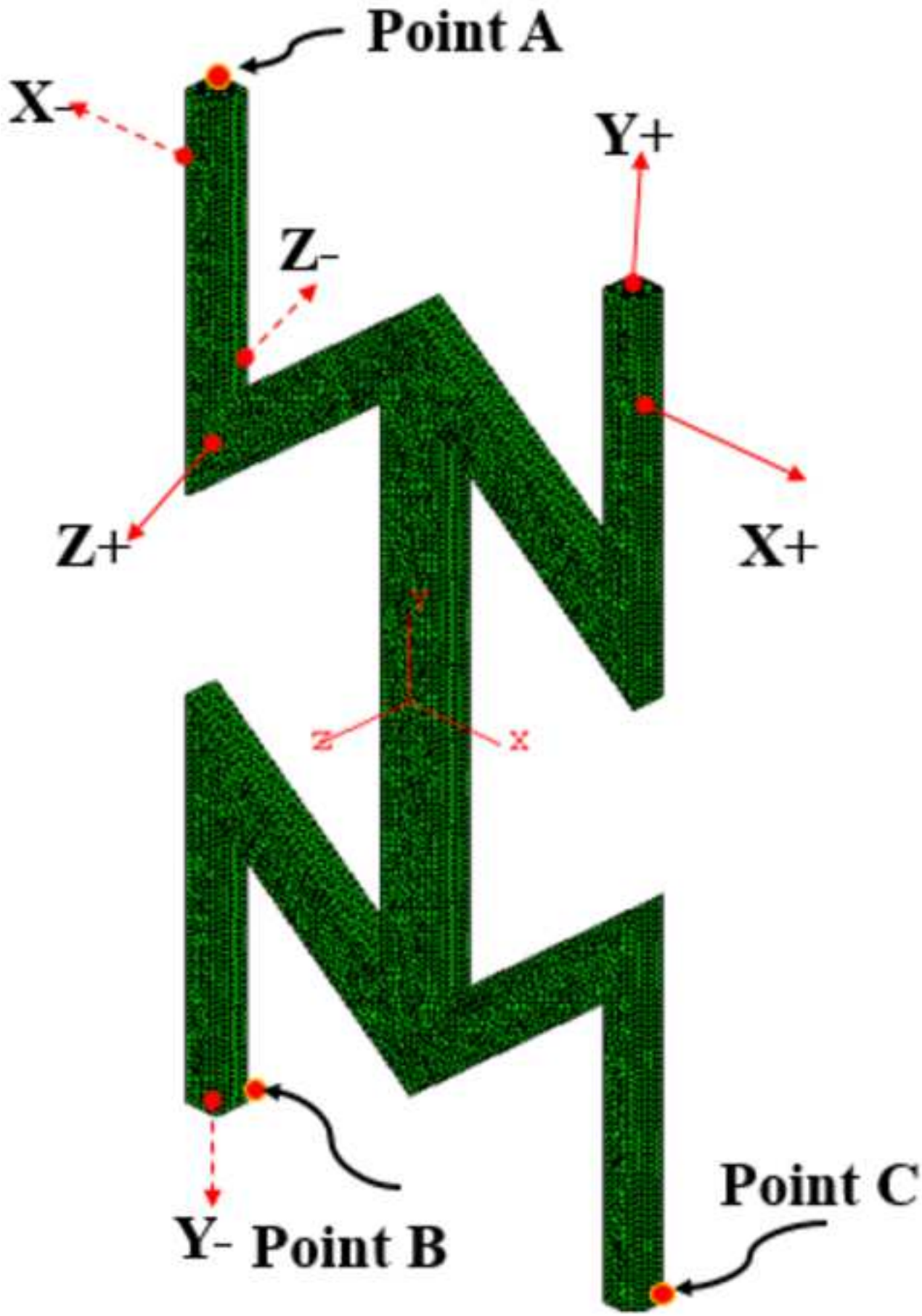

Figure

Click here to access/download;Figure;Figure3.tiff

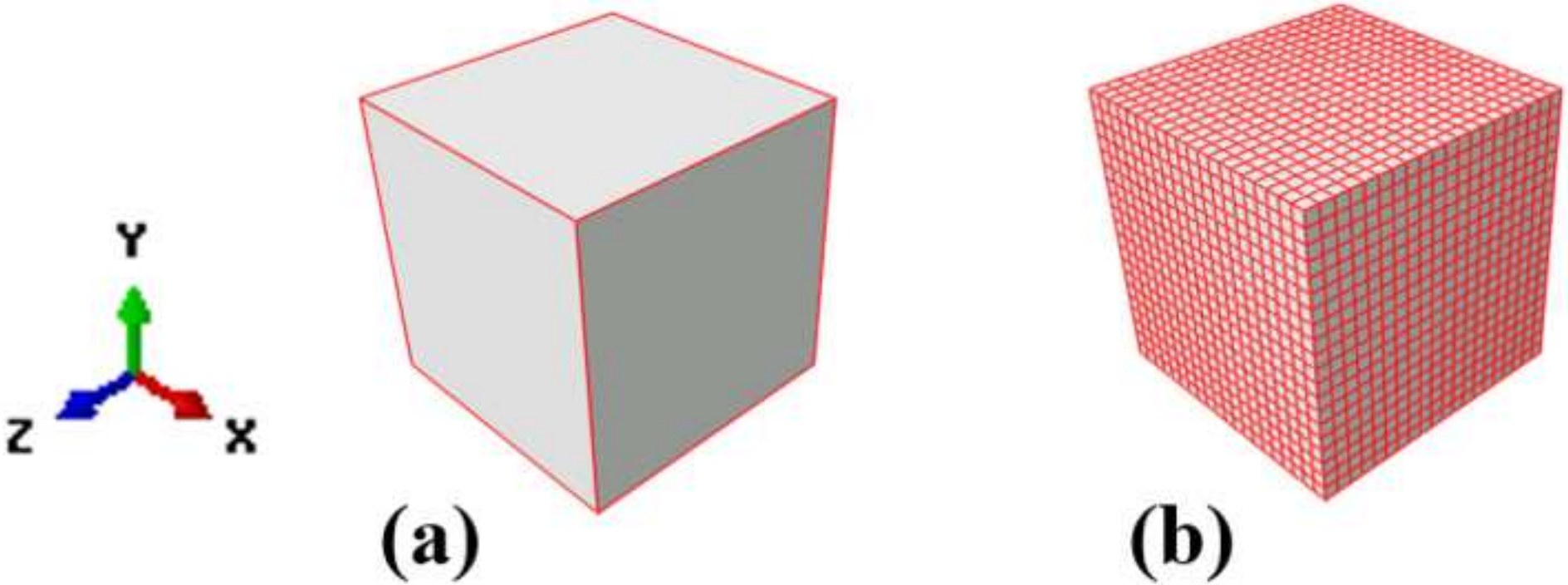

Figure

Click here to access/download;Figure;Figure4.tiff

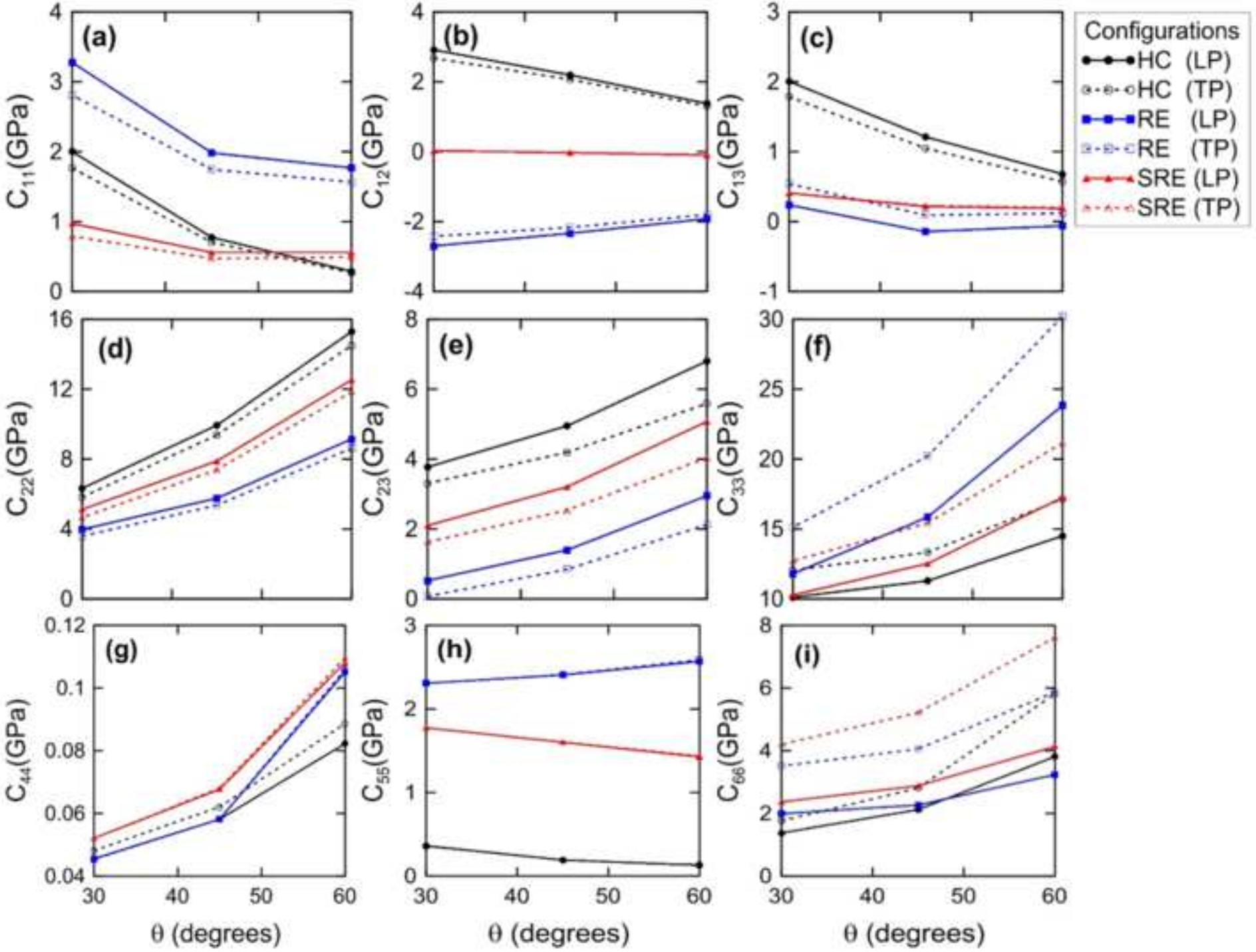

Figure

Click here to access/download;Figure;Figure5.tiff

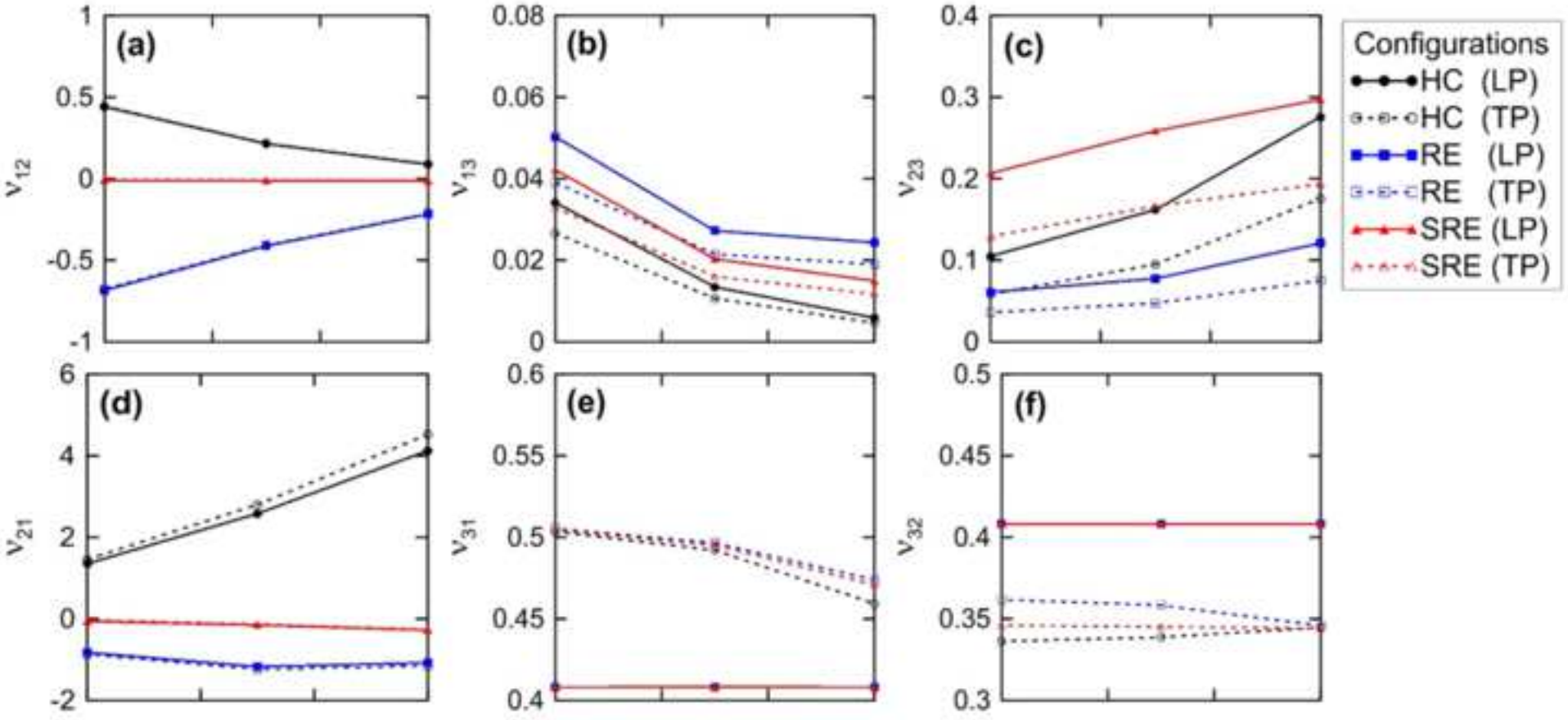

Figure

Click here to access/download;Figure;Figure6.tiff

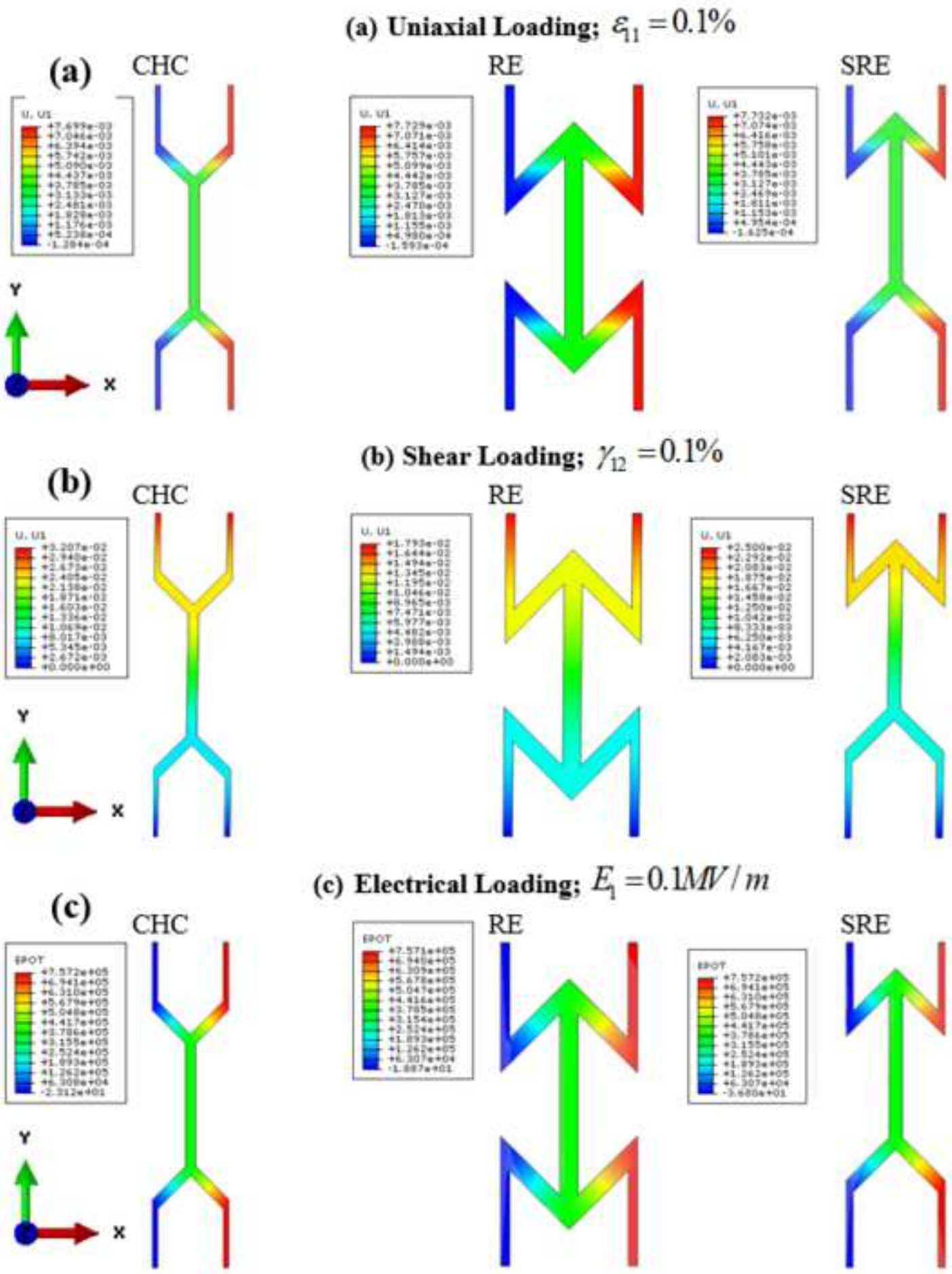

Figure

Click here to access/download;Figure;Figure7.tiff

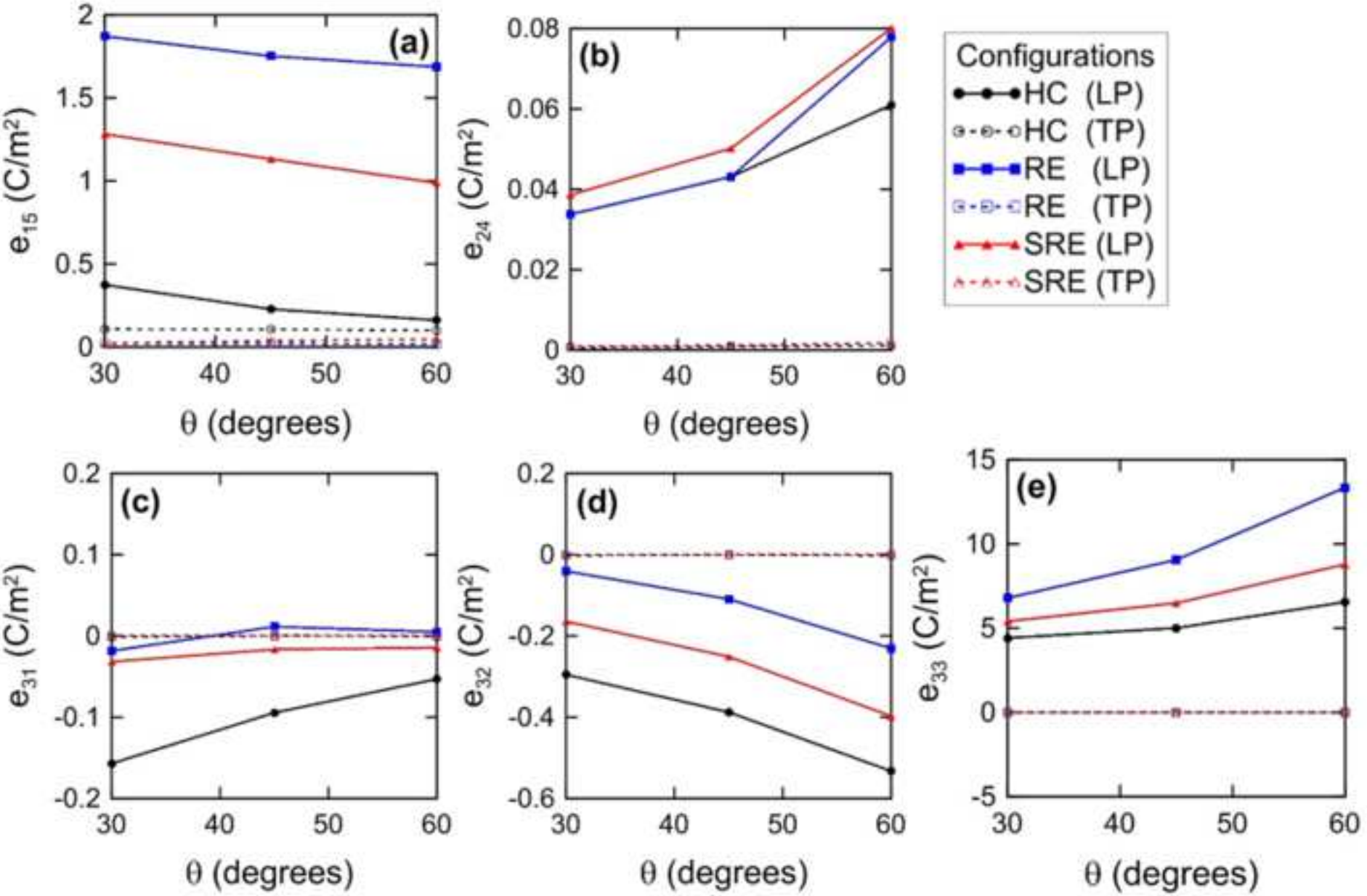

Figure

Click here to access/download;Figure;Figure8.tiff

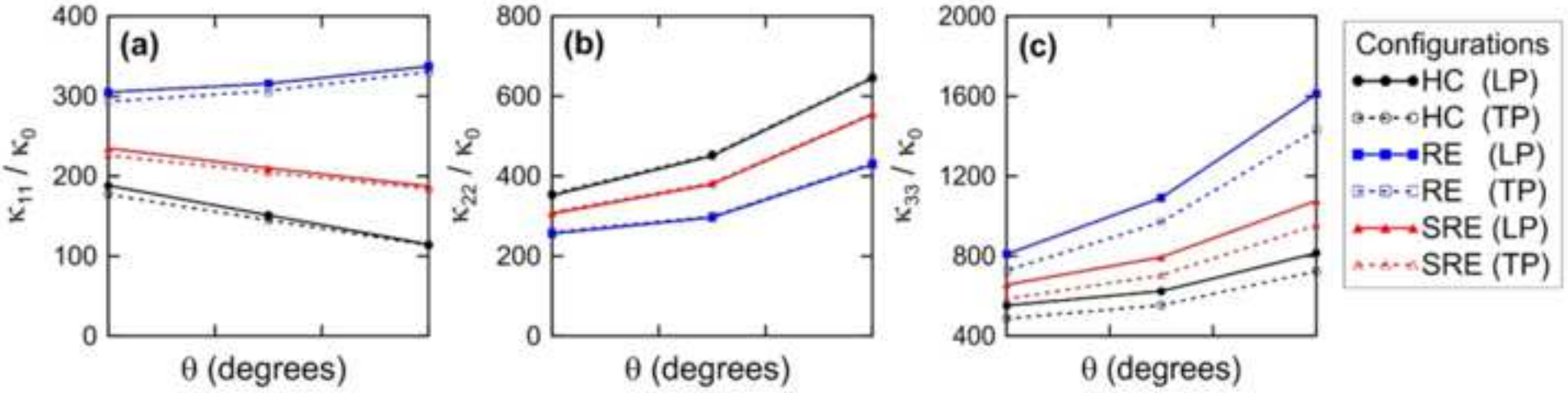

Figure

Click here to access/download;Figure;Figure9.tiff

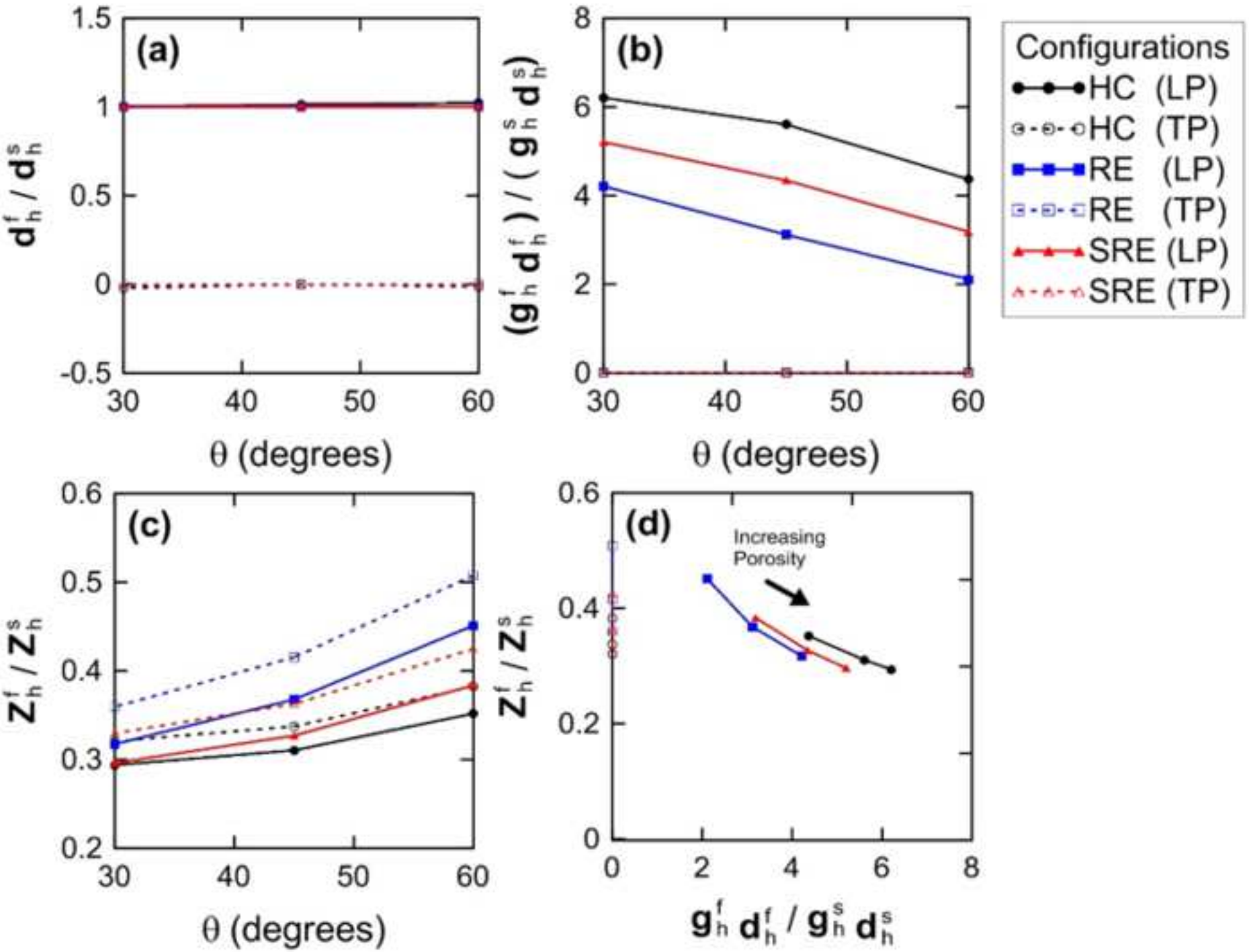

Figure

Click here to access/download;Figure;Figure10.tiff

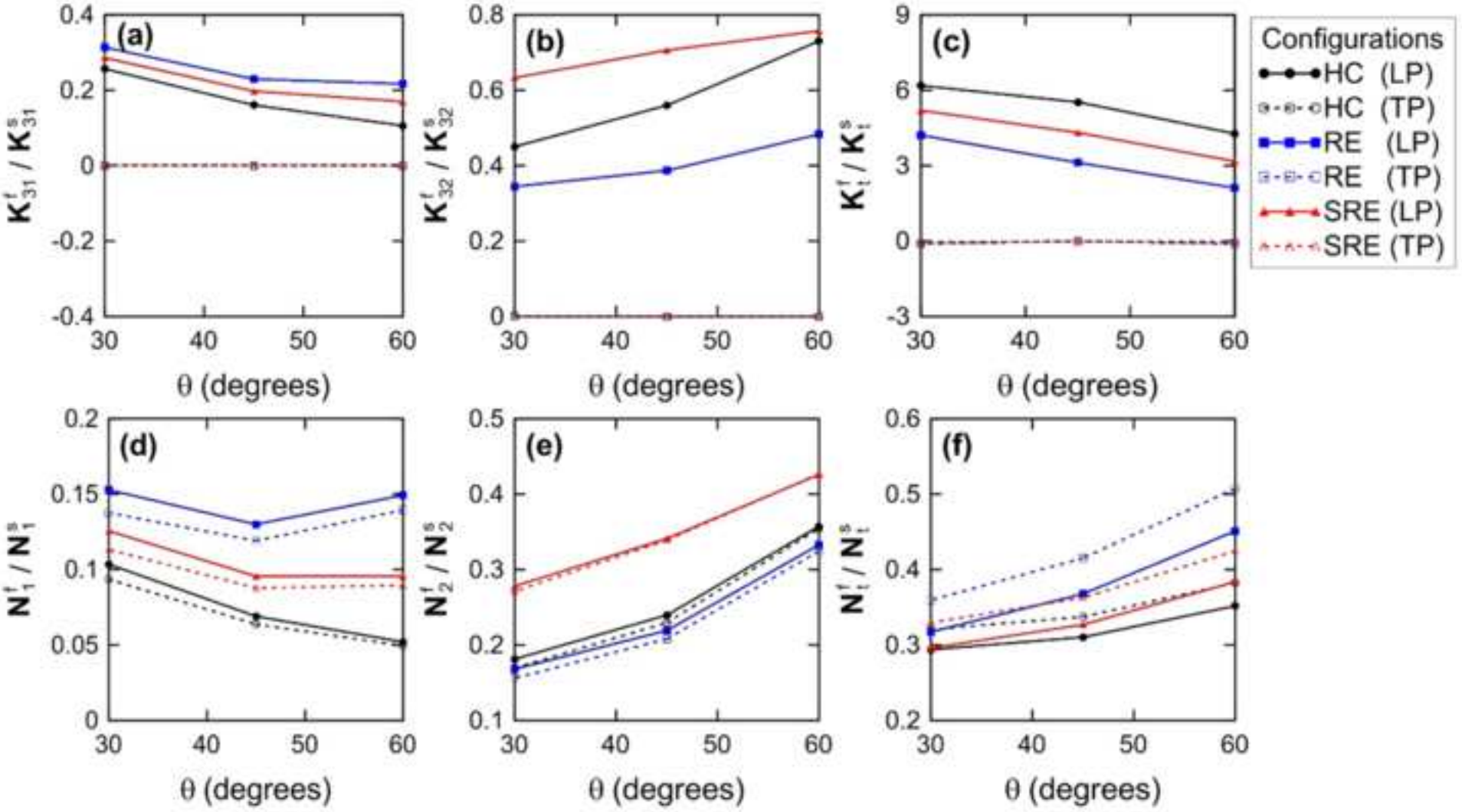

Figure 1 Piezoelectric hexagonal HC cellular networks with their unit cells a) Conventional hexagonal HC structure (CHC) b) a re-entrant HC (RE) c) semi-re-entrant HC (SRE).

Figure 2 The unit cell of HC RE meshed with 10 node quadratic tetrahedron piezoelectric elements (C3D10E) showing 6 boundary faces with respect to the axes directions.

Figure 3: Sanity Check with a) one element and b) 100x100x100 elements.

Figure *4*: The overall elastic constants of piezoelectric HC cellular network at various angles (30^o, 45^o, 60^o).

Figure 5: Variation in the overall Poisson's ratio with various angles (30^o, 45^o, 60^o) for piezoelectric HC networks.

Figure 6 Displacement and electric potential contours in the UCs of several classes of piezoelectric HC foam structures with angle 45^o. a) Displacement contours under mechanical normal loading (i.e., 0.1% normal strain along the x-axis) b) Displacement contours under mechanical shear loading (i.e., 0.1% shear strain in the x-y plane). c) Electric potential contours under electric field of 0.1MV/m.

Figure 7: The overall piezoelectric constants of HC cellular network at various angles (30^o, 45^o, 60^o).

Figure 8: The overall dielectric constants of HC cellular network at various angles (30^o, 45^o, 60^o).

Figure 9: Normalized FOMs of HC cellular network at various angles (30^o, 45^o, 60^o). (a) hydrostatic strain coefficient, (b) hydrostatic figure of merit, (c) acoustic impedance (d) Z-d_h.g_h relation

Figure 10: Selected normalized FOMs of HC cellular network at various angles (30^o, 45^o, 60^o).

Copyright Agreement
Click here to access/download;Copyright Agreement;Signed-CTA-form.pdf

ASCE Authorship, Originality, and Copyright Transfer Agreement

Publication Title: Piezoelectric Metamaterial with Negative and Zero Poisson's Ratio

Manuscript Title: Piezoelectric Metamaterial with Negative and Zero Poisson's Ratio

Author(s) – **Names, postal addresses, and e-mail addresses of all authors**

Kamran A. Khan, PO Box 127788, Abu Dhabi UAE

Sara Al Mansoor, PO Box 127788, Abu Dhabi UAE

Sohaib Z. Khan, Department of Mechanical Engineering, Islamic University of Madinah, Madinah, Saudi Arabia

Muhammad Ali Khan, School of Aerospace, Transport and Manufacturing, Cranfield University, UK

I. Authorship Responsibility

To protect the integrity of authorship, only people who have significantly contributed to the research or project and manuscript preparation shall be listed as coauthors. The corresponding author attests to the fact that anyone named as a coauthor has seen the final version of the manuscript and has agreed to its submission for publication. Deceased persons who meet the criteria for coauthorship shall be included, with a footnote reporting date of death. No fictitious name shall be given as an author or coauthor. An author who submits a manuscript for publication accepts responsibility for having properly included all, and only, qualified coauthors.

I, the corresponding author, confirm that the authors listed on the manuscript are aware of their authorship status and qualify to be authors on the manuscript according to the guidelines above.

Kamran A Khan	Kakhan	29-01-2019
Print Name	Signature	Date

II. Originality of Content

ASCE respects the copyright ownership of other publishers. ASCE requires authors to obtain permission from the copyright holder to reproduce any material that (1) they did not create themselves and/or (2) has been previously published, to include the authors' own work for which copyright was transferred to an entity other than ASCE. Each author has a responsibility to identify materials that require permission by including a citation in the figure or table caption or in extracted text. Materials re-used from an open access repository or in the public domain must still include a citation and URL, if applicable. At the time of submission, authors must provide verification that the copyright owner will permit re-use by a commercial publisher in print and electronic forms with worldwide distribution. For Conference Proceeding manuscripts submitted through the ASCE online submission system, authors are asked to verify that they have permission to re-use content where applicable. Written permissions are not required at submission but must be provided to ASCE if requested. Regardless of acceptance, no manuscript or part of a manuscript will be published by ASCE without proper verification of all necessary permissions to re-use. ASCE accepts no responsibility for verifying permissions provided by the author. Any breach of copyright will result in retraction of the published manuscript.

I, the corresponding author, confirm that all of the content, figures (drawings, charts, photographs, etc.), and tables in the submitted work are either original work created by the authors listed on the manuscript or work for which permission to re-use has been obtained from the creator. For any figures, tables, or text blocks exceeding 100 words from a journal article or 500 words from a book, written permission from the copyright holder has been obtained and supplied with the submission.

Kamran A Khan	Kakhan	29-01-2019
Print name	Signature	Date

III. Copyright Transfer

ASCE requires that authors or their agents assign copyright to ASCE for all original content published by ASCE. The author(s) warrant(s) that the above-cited manuscript is the original work of the author(s) and has never been published in its present form.

The undersigned, with the consent of all authors, hereby transfers, to the extent that there is copyright to be transferred, the exclusive copyright interest in the above-cited manuscript (subsequently called the "work") in this and all subsequent editions of the work (to include closures and errata), and in derivatives, translations, or ancillaries, in English and in foreign translations, in all formats and media of expression now known or later developed, including electronic, to the American Society of Civil Engineers subject to the following:

- The undersigned author and all coauthors retain the right to revise, adapt, prepare derivative works, present orally, or distribute the work, provided that all such use is for the personal noncommercial benefit of the author(s) and is consistent with any prior contractual agreement between the undersigned and/or coauthors and their employer(s).
- No proprietary right other than copyright is claimed by ASCE.
- If the manuscript is not accepted for publication by ASCE or is withdrawn by the author prior to publication (online or in print), or if the author opts for open-access publishing during production (journals only), this transfer will be null and void.
- Authors may post a PDF of the ASCE-published version of their work on their employers' ***Intranet*** with password protection. The following statement must appear with the work: "This material may be downloaded for personal use only. Any other use requires prior permission of the American Society of Civil Engineers."
- Authors may post the ***final draft*** of their work on open, unrestricted Internet sites or deposit it in an institutional repository when the draft contains a link to the published version at www.ascelibrary.org. "Final draft" means the version submitted to ASCE after peer review and prior to copyediting or other ASCE production activities; it does not include the copyedited version, the page proof, a PDF, or full-text HTML of the published version.

Exceptions to the Copyright Transfer policy exist in the following circumstances. Check the appropriate box below to indicate whether you are claiming an exception:

☐ **U.S. GOVERNMENT EMPLOYEES:** Work prepared by U.S. Government employees in their official capacities is not subject to copyright in the United States. Such authors must place their work in the public domain, meaning that it can be freely copied, republished, or redistributed. In order for the work to be placed in the public domain, ALL AUTHORS must be official U.S. Government employees. If at least one author is not a U.S. Government employee, copyright must be transferred to ASCE by that author.

☐ **CROWN GOVERNMENT COPYRIGHT:** Whereby a work is prepared by officers of the Crown Government in their official capacities, the Crown Government reserves its own copyright under national law. If ALL AUTHORS on the manuscript are Crown Government employees, copyright cannot be transferred to ASCE; however, ASCE is given the following nonexclusive rights: (1) to use, print, and/or publish in any language and any format, print and electronic, the above-mentioned work or any part thereof, provided that the name of the author and the Crown Government affiliation is clearly indicated; (2) to grant the same rights to others to print or publish the work; and (3) to collect royalty fees. ALL AUTHORS must be official Crown Government employees in order to claim this exemption in its entirety. If at least one author is not a Crown Government employee, copyright must be transferred to ASCE by that author.

☐ **WORK-FOR-HIRE:** Privately employed authors who have prepared works in their official capacity as employees must also transfer copyright to ASCE; however, their employer retains the rights to revise, adapt, prepare derivative works, publish, reprint, reproduce, and distribute the work provided that such use is for the promotion of its business enterprise and does not imply the endorsement of ASCE. In this instance, an authorized agent from the authors' employer must sign the form below.

☐ **U.S. GOVERNMENT CONTRACTORS:** Work prepared by authors under a contract for the U.S. Government (e.g., U.S. Government labs) may or may not be subject to copyright transfer. Authors must refer to their contractor agreement. For works that qualify as U.S. Government works by a contractor, ASCE acknowledges that the U.S. Government retains a nonexclusive, paid-up, irrevocable, worldwide license to publish or reproduce this work for U.S. Government purposes only. This policy DOES NOT apply to work created with U.S. Government grants.

I, the corresponding author, acting with consent of all authors listed on the manuscript, hereby transfer copyright or claim exemption to transfer copyright of the work as indicated above to the American Society of Civil Engineers.

Kamran A Khan

Print Name of Author or Agent

29-01-2019

Signature of Author of Agent Date

More information regarding the policies of ASCE can be found at http://www.asce.org/authorsandeditors

Response to Reviewers Comments
Click here to access/download;Response to Reviewers Comments;2-JEM_Response_to_Reviewers_rev1.docx

Taryn Dollings
Editorial Coordinator
Materials Research Bulletin

January 23, 2018

Subject: Revised Manuscript Ref.: Ms. No. EMENG-4328 and responses to the reviewers' comments:

"Piezoelectric Metamaterial with Negative and Zero Poisson's Ratio"
Authors: Kamran A Khan; Sara Al Mansoor; Sohaib Zia Khan; Muhammad Ali Khan

Dear Taryn Dollings,

Enclosed with this letter, please find a detailed response to the reviewers' comments and how these comments are addressed.

Major revisions in the revised manuscript as per reviewers' suggestions:

- The introduction has been revised and many relevant and recent papers are cited with detailed discussions on
    - Why does Auxetic geometry truly matters?
    - linearized electromechanical coupled constitutive relations.

All the major modifications are highlighted with red color text.

Please do not hesitate to contact if you need any additional information.

Sincerely,

Kamran A. Khan, Ph.D.
Assistant Professor
Department of Aerospace Engineering
Khalifa University of Science and Technology
PO Box 127788, Abu Dhabi, UAE
T +971 (0)2 401 8227
F +971 (0)2 447 2442
kamran.khan@ku.ac.ae

Response to Reviewer' comments:

We would like thank the referees for their kind and constructive comments that have enabled us to clarify some important points overlooked in the original manuscript. Taking the referees' comments into consideration, we have revised the manuscript to our best. All changes are highlighted by red color text in the revised manuscript
The responses to reviewer's comments are listed below:

Comments to the Author
-Reviewer 1
This is a nice study on the Piezoelectric Metamaterial with Negative and Zero Poisson's Ratio. They used auxetic geometries to enhance the properties of piezoelectric composites. The mechanics part is nicely done. It can be published after these major comments:

Response: The authors would like to thank the reviewer for appreciating our work.

1- Piezoelectric materials are light. Why does auxectic geometry truly matter?
Response:
To address reviewer's concern on why the auxetic geometry really matter, the following paragraph has been added in the revised manuscript.

Several researchers have shown that the auxetic geometry enhances the performance of the piezocomposite and porous piezoelectric materials. Smith [1] showed that the negative Poisson's ratio polymer matrix enhances the performance of the piezocomposite materials. Numerous researchers employed topology optimization techniques and the homogenization method to improve the performance of piezocomposite materials by designing new topologies of unit cells. Sigmund et al [2] employed the topology optimization method suggested by Bendsøe and Kikuchi [3] to design 1-3 piezocomposites with optimal performance characteristics for hydrophone applications. When design for maximum d_h and $d_h.g_h$, the optimal three-dimensional, anisotropic porous matrix microstructure found to possess negative Poisson's ratios in certain directions similar to re-entrant honeycomb network. Sigmund et al [2] showed that optimized porous microstructure design enhances the values of d_h and $d_h.g_h$ over pure piezoceramics by factors of more than 10 and 10,000, respectively. Silva, Kikuchi, and co-workers [4], [5] proposed a topology optimization techniques of finding the distribution of material and voids phases in a periodic unit cell that optimizes piezocomposite electromechanical efficiency. Several porous 2D and 3D piezoelectric-polymer and piezoelectric cellular microstructure were also proposed with negative Poisson's ratio behavior.

2- Along the same line, does the geometry and cell design help strength (the enhancement is electric properties are good not magnificent)? In fact, these designs can create certain stress concentration and reduce the strength, which makes it impractical. Please comment.

Response:

For the proposed piezoelectric honeycomb cellular networks, by varying the re-entrant angle, a wide range of tunable elastic, piezoelectric and dielectric properties can be obtained that cannot be realized by monolithic piezoelectric materials. Since electromechanical properties exhibit individual dependence on an angle so they cannot all be optimized at once, though an optimum combination of properties can be obtained. For example, using topology optimization (Sigmund et al. [2]) the cell design should be optimized such that it gives the required strength and electromechanical properties. The proposed 3-1 type piezoelectric cellular networks are limited in terms of their electromechanical properties and strength. Recently, we have shown that 3-3 type piezoelectric metamaterials can provide a good combination of strength and electromechanical properties [6]. In fact, the 3-3 type piezoelectric porous metamaterials design enhances the values of d_h and $d_h.g_h$ over pure piezoceramics by factors of more than 15 and 12,000, respectively. In another study, using topology optimization, Sigmund et al [2] also showed that optimized porous microstructure design enhances the values of d_h and $d_h.g_h$ over pure piezoceramics by factors of more than 10 and 10,000, respectively.

This is true that the cellular lattice materials are prone to stress concentration regions but as discussed earlier the compromise in strength and electromechanical properties should be sought by the designer for the specific application and select the optimized design of cellular structure accordingly.

-Reviewer 2

Khan presents a finite-element based micromechanical modeling framework to compute the electromechanical properties of a series of periodic piezoelectric materials. Negative and zero Poisson's ratios were predicted based on averaged model. The work done in the paper is extensive, and the paper is well written with some revisions to be made before publication:

1. There are numerous grammatical errors and mistakes made in the paper.
   For example, line 101, it should be "described",
   line 11, "to" is to be removed,
   line 155, "total (of) four degree(s) of freedom..." is the correct form, and 2 commas are needed, one before "three" and one before "and",
   line 175 must be "poled" not "pole".
   Other lines that need corrections, among others, are line 196, 224, 257 (the figure number), 307, 308, 386, 387, 389, etc.

Response:

We appreciate the reviewer's careful review and thankful for suggested corrections. All corrections have been made. Manuscript is carefully revised with the help of an English language expert.

2. Authors have used linearized electromechanical coupled constitutive relations for the piezoelectric material being used. This formulation is generally accepted. Thereafter, the authors assume a similar form of constitutive relation, with averaged values, for the RVE that is build from the piezoelectric unit cell. This assumption leads to an orthotropic linear material model. We already know from the literature [1,2, 3] that linear microelements in an RVE will produce nonlinear behavior of the macro-material point. Even in the simplest case for the geometry shown in the paper, and for a linear isotropic material (and not a piezoelectric material), the geometry-driven non-linearity prevents the use of linear models as linear models do not correctly exhibit the complexity and inter-connectivity of different parameters involved in formulating the problem. Perhaps, a justification of using Eq. 2 in the paper will answer such objectives.

[1] Misra, A. and P. Poorsolhjouy, Granular micromechanics based micromorphic model predicts frequency band gaps. Continuum Mechanics and Thermodynamics, 2016. 28(1-2): p. 215-234.
[2] Rosi, G. and N. Auffray, Anisotropic and dispersive wave propagation within strain-gradient framework. Wave Motion, 2016. 63: p. 120-134.
[3] dell'Isola, F., et al., Pantographic metamaterials: an example of mathematically driven design and of its technological challenges. Continuum Mechanics and Thermodynamics, 2018: p. 1-34.

Response:

Thanks for providing the above references. We appreciate the reviewer's recommendation and found it useful for our research. To address the reviewer's concern, we have added a small paragraph discussing the role of linearized electromechanical coupled constitutive relations in designing piezocomposites and porous piezoelectric materials. We have cited the above mentioned reference and many relevant and recent papers in the revised manuscript.

To address reviewer's concern, the following text has been added in the revised manuscript.

We considered the linearized electromechanical coupled constitutive relations for each ligament material to obtain the homogenization electromechanical properties of the proposed cellular network. These linearized constitutive relations are simple, attractive and, arguably, the most feasible approach for describing the electromechanical response of a cellular network at the macroscale [7],[8],[9],[2]. These assumptions lead to an orthotropic linear electromechanical material model. However, there are advanced models available in the literature [[10], [11], [12]] that showed linear microelements in an RVE will produce a nonlinear homogenized response. The geometry-driven non-linearity prevents the use of linear models as linear models do not correctly exhibit the complexity and inter-connectivity of different parameters involved in formulating the problem. In the present study, we do not consider models that account for geometry-driven nonlinearity. However, it will be interesting to analyze the proposed cellular network using such advanced models that account for higher order gradient theory and geometry-driven non-linearity.

3. A consequence of the point mentioned in (2) is that the behavior of the material when excited will not be dispersive, while we know from [1] that dispersion occurs and the velocity of wave will be a function of the frequency/wavenumber. An explanation on this matter will also help the reader in grasping the physics of the problem.

Response:

The author's would like to thank the reviewer for raising this interesting point. The following text has been added in the revised manuscript discussing the behavior of material subjected to excitation while considering higher order gradient continuum models.

It should be emphasized here that the use of linearized electromechanical coupled constitutive relations has some implications. For example, higher order gradient continuum models have been recently used by several researchers to investigate the dispersive wave propagation in strain gradient elastic media. Contrary to classical elasticity within the strain gradient framework, Rosi and Auffray [11] showed that the wave propagation in hexagonal lattices becomes anisotropic and group velocity was proven to be different from energy velocity and should be treated as different quantities. Misra and Poorsolhjouy [10] derived a micro-morphic continuum

model for the elasticity of granular media and the dispersion graphs have presented showing the relationship between the micro-scale parameters and the dispersion behavior. Contrary to classical elasticity where all waves will be of an acoustic type and there will be no possibility of frequency band gaps, the micro-morphic continuum model has the capability to present band gaps over a large range of wave numbers. Their results indicate that there is a possibility of designing materials with specific wave propagation behaviors that can be used as alternates to piezoelectric materials used commonly for structural vibration control or for damage identification.

.

4. Line 185-186, how is forcing parallel faces of the unit cell to remain parallel justified? This extra boundary condition must be accounted for in the energy expressions. I suggest the authors clarify such an assumption further by stating the pros and cons of such an assumption.

Response:

We feel that this sentence is confusing and it does not explains clearly what we used in our computation. Here, the forcing of parallel faces of the unit cell to remain parallel is referred to only the faces subjected to displacement loading along one specific degree of freedom for load cases 1-6. The other faces follows the deformation mechanism as per the boundary conditions [13],[14],[15].

On the loading face, we use the common concept of master node to apply the boundary conditions. Here, the master node (the loading direction, e.g., displacement along x-axis for load case 1) is coupled with all the nodes on respective loading face along one degree of freedom. This coupling allows all the nodes to be displaced by the same amount as a master node. For the loading cases 7-9 there is no such conditions of forcing of parallel faces of the unit cell to remain parallel is considered.

To avoid confusion, we have removed the sentence on line 185-186.

Enforcing any additional boundary condition that has not been accounted in energy expression may lead to over- or under-stiff homogenized behavior of the unit cell and incorrect micro field variables distribution.

[1] W.A. Smith, Optimizing electromechanical coupling in piezocomposites using polymers with negative Poisson's ratio, in: IEEE 1991 Ultrason. Symp., 1991: pp. 661–666 vol.1. doi:10.1109/ULTSYM.1991.234109.
[2] O. Sigmund, S. Torquato, I.A. Aksay, On the design of 1–3 piezocomposites using topology optimization, J. Mater. Res. 13 (1998) 1038–1048.
[3] M.P. Bendsøe, N. Kikuchi, Generating optimal topologies in structural design using a homogenization method, Comput. Methods Appl. Mech. Eng. 71 (1988) 197–224.
[4] E.N. Silva, J.O. Fonseca, N. Kikuchi, Optimal design of piezoelectric microstructures, Comput. Mech. 19 (1997) 397–410.
[5] E.C.N. Silva, J.S.O. Fonseca, N. Kikuchi, Optimal design of periodic piezocomposites, Comput. Methods Appl. Mech. Eng. 159 (1998) 49–77.
[6] K.A. Khan, M.A. Khan, 3-3 piezoelectric metamaterial with negative and zero Poisson's ratio for hydrophones applications, Mater. Res. Bull. 112 (2019) 194–204. doi:10.1016/j.materresbull.2018.12.016.
[7] K.S. Challagulla, T.A. Venkatesh, Computational Modeling of Piezoelectric Foams, JOM. 65 (2013) 256–266.
[8] S. Iyer, M. Alkhader, T.A. Venkatesh, Electromechanical response of piezoelectric honeycomb foam structures, J. Am. Ceram. Soc. 97 (2014) 826–834.
[9] R. Kar-Gupta, T.A. Venkatesh, Electromechanical response of porous piezoelectric materials, Acta Mater. 54 (2006) 4063–4078.
[10] A. Misra, P. Poorsolhjouy, Granular micromechanics based micromorphic model predicts frequency band gaps, Contin. Mech. Thermodyn. 28 (2016) 215–234.
[11] G. Rosi, N. Auffray, Anisotropic and dispersive wave propagation within strain-gradient framework, Wave Motion. 63 (2016) 120–134.
[12] F. Dell'Isola, P. Seppecher, J.J. Alibert, T. Lekszycki, R. Grygoruk, M. Pawlikowski, D. Steigmann, I. Giorgio, U. Andreaus, E. Turco, Pantographic metamaterials: an example of mathematically driven design and of its technological challenges, Contin. Mech. Thermodyn. (2018) 1–34.
[13] K.A. Khan, R.K. Abu Al-Rub, Time dependent response of architectured Neovius foams, Int. J. Mech. Sci. 126 (2017) 106–119. doi:10.1016/j.ijmecsci.2017.03.017.
[14] K.A. Khan, R.K.A. Al-Rub, Modeling time and frequency domain viscoelastic behavior of architectured foams, J Eng Mech. 144 (2018) 1–15.
[15] S. Li, Boundary conditions for unit cells from periodic microstructures and their implications, Compos. Sci. Technol. 68 (2008) 1962–1974.

Cranfield University

CERES Research Repository **https://dspace.lib.cranfield.ac.uk/**

School of Aerospace, Transport and Manufacturing (SATM) Staff publications (SATM)

Piezoelectric metamaterial with negative and zero Poisson's ratios

Khan, K. A.

2019-09-28

Khan KA, Al Mansoor S, Khan SZ, Khan AK (2019) Piezoelectric metamaterial with negative and zero Poisson's ratios. Journal of Engineering Mechanics, Volume 145, Issue 12, December 2019 https://doi.org/10.1061/(ASCE)EM.1943-7889.0001674

Downloaded from CERES Research Repository, Cranfield University